Journal of Hazardous Materials 431 (2022) 128532

Contents lists available at ScienceDirect

Journal of Hazardous Materials

journal homepage: www.elsevier.com/locate/jhazmat

Research Paper

Arsenate and arsenite differential toxicity in *Tetrahymena thermophila*

Daniel Rodríguez-Martín [a], Antonio Murciano [b], Marta Herráiz [c], Patricia de Francisco [d], Francisco Amaro [c], Juan Carlos Gutiérrez [c], Ana Martín-González [c], Silvia Díaz [c,*]

[a] Animal Health Research Centre (CISA), National Institute for Agricultural and Food Research and Technology (INIA-CSIC), 28130 Madrid, Spain
[b] Department of Biodiversity, Ecology and Evolution, Faculty of Biology, Complutense University of Madrid, Spain
[c] Department of Genetics, Physiology and Microbiology, Faculty of Biology, Complutense University of Madrid, Spain
[d] Astrobiology Center (INTA-CSIC), Carretera de Ajalvir Km 4, 28850 Madrid, Spain

HIGHLIGHTS

- Unlike mammals, in *Tetrahymena,* arsenate is much more toxic than arsenite.
- The lethal effects of arsenic binary mixtures show an additive effect.
- As(III) causes an adipotropic effect, As (V) induces mitophagy and both originate ROS/RNS.
- Mitochondria are one of the main targets of As(V) adverse effects.
- Thioredoxin, glutathione metabolism and metallothioneins are involved in detoxification response.

GRAPHICAL ABSTRACT

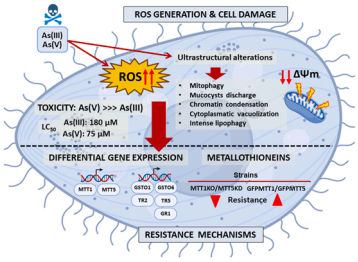

ARTICLE INFO

Editor: Youn-Joo An

Keywords:
Tetrahymena
Arsenite and arsenate
Toxicity
Mitochondrial dysfunction
Metallothioneins
Antioxidant gene expression

ABSTRACT

A comparative analysis of toxicities of both arsenic forms (arsenite and arsenate) in the model eukaryotic microorganism *Tetrahymena thermophila* (ciliate protozoa) has shown the presence of various detoxification mechanisms and cellular effects comparable to those of animal cells under arsenic stress. In the wild type strain SB1969 arsenate is almost 2.5 times more toxic than arsenite. According to the concentration addition model used in binary metallic mixtures their toxicities show an additive effect. Using fluorescent assays and flow cytometry, it has been detected that As(V) generates elevated levels of ROS/RNS compared to As(III). Both produce the same levels of superoxide anion, but As(V) also causes greater increases in hydrogen peroxide and peroxynitrite. The mitochondrial membrane potential is affected by both As(V) and As(III), and electron microscopy has also revealed that mitochondria are the main target of both arsenic ionic forms. Fusion/fission and swelling mitochondrial and mitophagy, together with macroautophagy, vacuolization and mucocyst extruction are mainly associated to As(V) toxicity, while As(III) induces an extensive lipid metabolism dysfunction (adipotropic effect). Quantitative RT-PCR analysis of some genes encoding antioxidant proteins or enzymes has shown that glutathione and thioredoxin metabolisms are involved in the response to arsenic stress. Likewise, the

Abbreviations: AFU, arbitrary fluorescence units; CCCP, carbonyl cyanide m-chlorophenyl-hydrazone; DHR123, dihydrorhodamine 123; GFP, green fluorescent protein; GSH, glutathione; GR, glutathione reductase; GST, Glutathione-S-transferases; HE, dihydroethidium; IP, iodine propidium; JC-1, 5,5′,6,6′-tetrachloro-1,1′,3,3′-tetraethylbenzimidazolcarbocyanide iodide; Ma, macronucleus; Mi, micronucleus; MT, metallothionein; RNS, reactive nitrogen species; ROS, reactive oxygen species; TR, thioredoxin reductases.

* Correspondence to: Department of Genetics, Physiology and Microbiology, Faculty of Biology, Complutense University of Madrid, C/. José Antonio Novais 12, 28040 Madrid, Spain.

E-mail addresses: rodriguez.daniel@inia.es (D. Rodríguez-Martín), murciano@bio.ucm.es (A. Murciano), marthe09@ucm.es (M. Herráiz), pdefrancisco@cab.inta-csic.es (P. de Francisco), famaroto@ucm.es (F. Amaro), jcgutier@ucm.es (J.C. Gutiérrez), anamarti@ucm.es (A. Martín-González), silviadi@ucm.es (S. Díaz).

https://doi.org/10.1016/j.jhazmat.2022.128532
Received 2 January 2022; Received in revised form 9 February 2022; Accepted 18 February 2022
Available online 25 February 2022

function of metallothioneins seems to be crucial in arsenic detoxification processes, after using both metallothionein knockout and knockdown strains and cells overexpressing metallothionein genes from this ciliate. The analysis of the differential toxicity of As(III) and As(V) shown in this study provides cytological and molecular tools to be used as biomarkers for each of the two arsenic ionic forms.

1. Introduction

Arsenic (As) is a non-essential metalloid, widely distributed in the environment and ranking 12th in abundance in the earth's crust (Burwell, 2014; Shaji et al., 2021). The main natural sources of arsenic in the environment are volcanic activity and natural volatilization of organic arsenic compounds in soils (Mukhopadhyay and Rosen, 2002). Humans have significantly contributed to environmental pollution and recycling of this metalloid due to mining practices and industrial activities, such as metal smelting, electronics, dumping of chemical products, as well as metallurgy, glass industry, and armament (Brooks, 2007; Mandal and Suzuki, 2002).

In aquatic environments, arsenic is mainly found in two inorganic states; trivalent arsenic or arsenite As(III), which is usually found in groundwater, and pentavalent arsenic or arsenate As(V), that is the more stable form and negatively charged oxyanion at physiological pH (Nurchi et al., 2020; Shaji et al., 2021). On the other hand, in soils the arsenic species are more diverse including inorganic, organic forms and arsenic-containing minerals (Al-Makishah et al., 2020). In humans, the most important exposure to arsenic is through ingestion of arsenic contaminated food and water (Jomova et al., 2011; Nurchi et al., 2020; Ozturk et al., 2021). It has been estimated that in more than 180 countries about 200–230 million people are at serious health risk for drinking groundwater with high arsenic levels (Shaji et al., 2021).

The arsenic toxicity has been intensively analyzed in microorganisms, plants, animals and especially in humans (Bali and Sidhu, 2021; Byeon et al., 2021; Mazumber et al., 2020; Ozturk et al., 2021). In most of the studied species, As(III) is more biotoxic than As(V), although there are remarkable differences (Rahman and Hassler, 2014; Byeon et al., 2021). As arsenic is not an essential element for the cell, there are no specific carriers that incorporate it into the cell, so in many cells the entry of this metalloid is by using essential metal transporters (Dhuldhaj et al., 2013; Garbinski et al., 2019; Tsai et al., 2009). The mechanisms of arsenic toxicity are complex and not fully understood (Hu et al., 2020). Like other non-essential metal(loid)s (Cd, Hg), the arsenic toxicity is due to the concurrence of several negative effects caused by its interaction with the main target biomolecules (proteins, lipids, DNA) (Ozturk et al., 2021). Many experimental evidences indicate that ROS (Reactive Oxygen Species) and RNS (Reactive Nitrogen Species) are generated after arsenic exposure in animals and plants, which induces direct oxidative damage to biomolecules, altering several cell organelles, signaling pathways and generating epigenetic modifications (Hughes, 2002; Flora, 2011; Hu et al., 2020). It is well known that arsenic exposure, in addition to ROS production, can originates alterations in cellular proteostasis. As(III) can bind to the -SH groups of cysteines disrupting the correct protein folding, and altering the biological activity or structural role of them (Finnegan and Chen, 2012; Tam and Wang, 2020). As(V) can generate an intracellular imbalance of phosphate by substituting it in phosphorylation reactions, and the most important consequence of this is the oxidative phosphorylation uncoupling, thus inhibiting the energy-linked NAD reduction, mitochondrial respiration and ATP synthesis (Hughes, 2002; Prakash et al., 2015). Many in vitro and in vivo studies report the mutagenicity and genotoxicity of inorganic arsenic compounds (Al-Zoughool et al., 2019; Jomova et al., 2011). Mutagenicity by this metalloid comes from its ability of interfering with the DNA repairing system (Tam et al., 2020).

Due to its high toxicity, living beings have developed different strategies to detoxify arsenic (De Francisco et al., 2021). One of the most usual tools against toxic metal(loid)s, mainly in eukaryotic cells, is the blocking of these ions by proteins or peptides rich in cysteine residues. These include metallothioneins (MTs), phytochelatins (PCs) and glutathione tripeptide (GSH) (Balzano et al., 2020; Carrillo and Borthakur, 2021; De Francisco et al., 2018, 2021; Gutierrez et al., 2019). Chelation and bioaccumulation of As (III) or As(V) mediated by MTs and/or PCs have been reported in microorganisms, animals and plants (Kumari et al., 2018; Pan et al., 2018; Rahman and De Ley, 2017). Likewise, arsenic biosorption can be carried out by both living and dead cells since these ions can be immobilized by surface cellular exopolymers. This strategy has been reported as a tolerance-resistance mechanism in microalgae (Leong and Chang, 2020). Arsenic biotransformation is one of the most studied cellular detoxification processes (Stolz et al., 2002). Two main mechanisms have been described: As(III) or As(V) enzymatic methylation (Di et al., 2019; Hirano, 2020; Thomas, 2021), and reduction of arsenate to arsenite, which is then ejected from the cell by an arsenite-specific efflux pump (Stolz et al., 2006). One of the most common cellular detoxification systems for both inorganic and organic arsenicals is the expulsion of these toxicants by efflux pumps from the cytoplasm to the cell outside (Garbinski et al., 2019; Maciaszczyk-Dziubinska et al., 2012; Rahman and Hassler, 2014). In addition, as an direct or indirect defense mechanism against arsenic, there is a set of enzymatic (superoxide dismutase, glutathione peroxidase, catalase, glutharedoxin, gluthatione transferases, glutathione or thioredoxin reductases, among others) and non-enzymatic molecules (glutathione, metallothioneins, phytochelatins, etc.) involved in neutralizing or minimizing the formation of ROS or RNS and preventing oxidative stress. (Bali and Sidhu, 2021; Hayes et al., 2005; Hu et al., 2020; Kumar et al., 2016).

The main aim of this research work is to perform a comparative evaluation between both forms of arsenic, As(III) and As(V), in the ciliate protozoan *Tetrahymena thermophila*. This is a eukaryotic microorganism model widely used in ecotoxicology due to its similarities with animal cells (Gutierrez et al., 2008). In addition, there is a need to increase our current knowledge of the effects of these inorganic pollutants on ciliates, microorganisms widely distributed in many different ecosystems. This study involves a toxicological evaluation of As(III) or As (V) and their binary mixtures using the wild-type strain, strains overexpressing MT genes, and MT knockout and knockdown strains obtained from this ciliate (Amaro et al., 2014; De Francisco et al., 2017). ROS/NRS generation and mitochondrial membrane potential assessments, an ultrastructural cellular analysis and a differential gene expression study of genes encoding selected antioxidant biomolecules were carried out.

2. Materials and methods

2.1. Strains and culture conditions

We used a wild-type strain (SB1969) of *Tetrahymena thermophila*, kindly supplied by Dr. E. Orias (University of California, Santa Barbara, USA). In addition, two strain of *Tetrahymena thermophila* GFPMTT1 and GFPMTT5, which contain multicopy plasmids bearing the constructs *PMTT1::GFP::MTT1* or *PMTT1::GFP::MTT5*, which overexpress *MTT1* or *MTT5* genes, respectively. These plasmidic constructs carry the promoter of the Cd-metallothionein *MTT1* gene fused to the *GFP* (Green Fluorescent Protein) reporter gene and the ORF of each MT gene isoform *MTT1* or *MTT5* (Amaro et al., 2014). Also, two genetically modified strains of *T. thermophila* were used in this study; MTT1KO (knockout for *MTT1* gene) and MTT5KD (knockdown for *MTT5* gene) strains (De

Francisco et al., 2017).

Cells were axenically grown in PP210 medium [2% w/v proteose peptone (Pronadisa-Condalab,1607), supplemented with 10 μM $FeCl_3$ and 250 μg/mL of streptomycin sulphate (Calbiochem, 3810–74–0) and penicillin G (Sigma-Aldrich, 69–57–8), and maintained at a constant temperature of 30 ± 1 °C. Paromomycin sulphate (Sigma-Aldrich, 1263–89–4) (2 μg/mL) was added to maintain the multi-copy plasmid in GFPMTT1 and GFPMTT5 strains. MTT5KD strain is inherently unstable, because without selective pressure the *MTT5* gene copy number can increase. To prevent this, we maintained the cells in PP210 medium with 800 μg/mL of paromomycin.

2.2. Cytotoxicity bioassays

Log-phase cultures in PP210 medium (1–3 $\times 10^5$ cells/mL) of *T. thermophila* SB1969 (wild-type strain) and genetically modified strains (GFPMTT1, GFPMTT5, MTT1KO and MTT5KD) were harvested by centrifugation (3 min at 2000 rpm) and washed with TrisHCl buffer 0.01 M (pH 6.8). Cellular suspensions were distributed in different tubes (1 mL/tube) and exposed to a series of increasing concentrations of arsenite or arsenate (24 h treatments at 30º C). The concentrations of As (III) or As(V) used were selected based on LC_{50} values, both below and exceeding these values, depending on the type of study and to obtain a more diverse cellular response. Cytotoxic effects were estimated at 24 h of treatment, based on the cell cycle of this ciliated protozoan. Arsenite was tested as sodium (meta) arsenite ($NaAsO_2$, Sigma-Aldrich, 7784–46–5) and arsenate as sodium arsenate dibasic heptahydrate (Na_2HAsO_4. 7 H_2O. Sigma-Aldrich, 10048–95–0), solutions in 0.01 M Tris-HCl buffer (pH 6.8). To study the toxicity of binary mixtures of As (III) and As(V) in the wild-type strain of *T. thermophila* we used the Toxic Unit (TU) approach concentration addition model (Sprague, 1970). This model allows converting the concentrations used into TU values. Thus, the LC_{50} of As(III) or As(V) is assigned a value of 1 TU, half the concentration corresponding to the LC_{50} would be 0.5 TU, while the double of the LC_{50} would be 2 TU. The assays were design in such a way that the additive, synergistic (antagonistic or potentiation) effects could be assessed by trying 0.5, 1 or 2 TU of As(III) + As(V). An additive effect occurs when the sum of all metal TUs is 1 (the toxicity of the As(III) + As (V) mixture is the same as the individual As(III) or As(V) toxicities).

All fluorescent samples were assessed in a FACScalibur flow cytometer (Becton Dickinson) with Cell Quest software, equipped with an argon ion excitation laser (488 nm), forward scatter (FS) and side scatter (SS) detectors and four fluorescence detectors: FL1 (BP 530/30 nm), FL2 (585–542 nm), FL3 (LP 670 nm), FL4 (BP 616–661 nm). At least 5×10^3 cells per sample were collected and analysed in each assay. Red fluorescence due to propidium iodide (PI) (Sigma-Aldrich, 25535–16–4) fluorophore was quantifed by flow cytometry to estimate cell mortality (Romero et al., 2019). The probe PI (2.5 mg/mL) allows discriminating between viable non-fluorescent cells (PI-) and non-viable fluorescent cells with damaged or disrupted cell membranes (PI+). Fluorescent cells were detected in the FL3 channel. Three types of controls were used in each experiment: a calibrator sample (cells not exposed to metal or PI), a negative control or live cells (cells not exposed to metal but treated with PI), and the positive control or dead cells (cells pre-fixed with 37% formaldehyde and treated with PI) (Romero et al., 2019).

The PROBIT model (Bliss, 1935) and the statistical Statgraphics Centurion XVI and STATA 9.0 (confidence 95%, $p < 0.05$) have been used to calculate the lethal concentrations for killing 50% of the cells (median lethal concentration or LC_{50} parameter). Three independent experiments and copies from each of them were carried out to corroborated results.

2.3. Evaluation of ROS/RNS generation and mitochondrial membrane potential

To detect the intracellular formation of superoxides in control and treated cell populations we have used dihydroethidium (HE) (Sigma-Aldrich,104821–25–2), which is one of the most widely usual probes in animal cells (Gomes et al., 2005). HE stock solutions were made in dimethylsulfoxide (DMSO) (Sigma-Aldrich, 67–68–5) at 3 mM concentration. HE is oxidized by certain superoxides and other reactive species such as $ONOO^-$ (peroxinitrite) and OH^- (hydroxyl radical) (Gomes et al., 2005) to form ethidium (E^+) a fluorescent compound (excitation/emission at 520/610 nm) (Benov et al., 1998). Hydrogen peroxide (H_2O_2) assessment was made applying dihydrorhodamine 123 (DHR123) (Biotium, 109244–58–8) at 3 μg/mL final concentration (30 min treatment), which after oxidation yields rhodamine 123, a green fluorescent lypophilic probe (excitation/emission at 505 /529 nm). DHR123 can be oxidized by H_2O_2, $ONOO^-$ or OH^- (Gomes et al., 2005; Kalyanaraman et al., 2014). Fluorescent cells were detected in the FL1 channel.

As(III) or As(V) effects on mitochondrial function were evaluated by applying the specific fluorochome JC-1 (5,5′,6,6′-tetrachloro-1,1′,3,3′-tetraethylbenzimidazolcarbocyanide iodide) (Calbiochem, 47729–63–5) at 50 μg/mL final concentration (30 min treatment). It is a lipophilic cationic dye that can selectively enter into mitochondria and reversibly change its colour from red to green as the mitochondrial membrane potential ($\Delta\psi_{mt}$) decreases. In healthy cells with high mitochondrial $\Delta\psi_{mt}$, JC-1 forms complexes known as J-aggregates with intense red fluorescence (absoption/emission at 585/590 nm) detected in FL2 channel. On the other hand, in apoptotic or unhealthy cells with low $\Delta\psi_{mt}$, JC-1 remains in monomeric form, showing a green fluorescence (absoption/emission at 510/527 nm) detected in the FL1 channel. The use of respiratory uncouplers, such as carbonyl cyanide m-chlorophenyl-hydrazone (CCCP) (Sigma-Aldrich, 555–60–2) causes quick mitochondrial membrane depolarization and this treatment can be used as a negative control.

2.4. Ultrastructural analysis by Transmission Electron Microscopy (TEM)

T. thermophila SB1969 strain cultures were exposed to 100 μM As(III) (24 h) or 30 μM As(V) (1 or 24 h) to analyze cell ultrastructural alterations. The TEM procedure described by Dentler (2000) was applied to controls and arsenic exposed populations. Ultrathin sections were stained with 2% uranyl acetate and lead citrate, mounted on copper grids and examined with a Jeol JEM 1010 transmission electron microscope operating at 75 kV. Detailed cell fixation and embedding procedures have been described in Díaz et al. (2016).

2.5. Total RNA isolation, cDNA synthesis and quantitative real-time RT-PCR

T. thermophila SB1969 cultures in exponential phase were exposed at As(III) 10 μM or As(V) 10 μM during 1 or 24 h. These concentrations are much lower than the LD_{50} values, to obtain the maximum number of viable cells. Cells were collected by centrifugation at 2000*g* for 2 min. Total RNA was isolated with TRI Reagent Solution (Ambion, Life Technologies, CA, USA, 108–95–2) according to manufacturer's protocol. To remove possible DNA contamination, samples were treated with DNase I (RNase free) (Ambion, 7732–18–5). RNA integrity was analyzed using denaturing 1.2% agarose gels according to Sambrook and Russell (2006), and sample concentrations were obtained by spectrophotometry using NanoDrop 1000 (Thermo Scientific). cDNA synthesis was carried out using 5 μg RNA, according to the protocol supplied by 1st Strand cDNA Synthesis kit (AMV, Roche). cDNA samples were amplified in duplicate in 96 microtiter plates. Each qPCR reaction (20 μL) contained: 10 μL of SYBR Green (Takara), 0.4 μL of ROX as passive reference dye (Takara), 1 μL of each primer (at 40 nM final concentration), 3.6 μL of ultrapure sterile water (Roche) and 4 μL of a 1/10 dilution of cDNA. PCR primers (Table S1) were designed using the "Primer Quest and Probe Design" online application from IDT (Integrated DNA Technologies). *ATUBQ* (α-tubulin) gene was used as an endogenous control or normalizer gene. Melting curves were obtained and primers specificity

was tested by confirming each PCR product by gel electrophoresis and sequencing. Real-time PCR reactions were carried out in an iQ5 real-time PCR apparatus (Bio-Rad) and the applied thermal cycling protocol was as follows: 5 min at 95 °C, 40 cycles (30 s at 95 °C, 30 s at 55 °C and 20 s at 72 °C), 1 min at 95 °C and 1 min at 55 °C. All controls [no template controls (NTC) and RT minus controls] were negative. The standard-curve parameters for each gene: amplification efficiency (E), slope (S) and correlation coefficient (R^2) are reported in Table S2. Results were processed by the stardard-curve method (Larionov et al., 2005), and were corroborated with at least two independent experiments, each performed in duplicate.

2.6. Statistical analysis

The software packages Statgraphics Centurion 16.0 and STATA 9.0, were used to obtain predictive models from experimental data. Mortality results from As(III) or As(V) were adjusted to a dosage-mortality sigmoid curve using the Probit model, and from it LC_{50}, LC_{10} and LC_{90} were estimated. Two-way ANOVA tests were carried out to study the effect of binary mixtures of As(III) and As(V). The experimental data from ROS assays with both HE and DHR123 flourochrome were adjusted to two logarithmic models, and two-way ANOVA test were performed. One-way Analysis of Variance test (ANOVA) were also carried out to assess significant differences between control and treated cells, and results were expressed as means ± standard error and p-value was fixed in < 0.05 for statistical significance. A two-way ANOVA and a Least Significant Difference (LSD) test were performed with mitochondrial membrane potential assays data to check differences between treatments and doses of As. Statistical analysis for qRT-PCR was carried out using the Pair Wise Fixed Reallocation Randomisation Test (REST-MCS β version 2 software) (Pfaffl et al., 2002). Prior to parametric tests performance, normal distribution (quantile-quantile plot and/or Shapiro-Wilk test) and homoscedasticity (F-test) for each data group was checked. Data in each group was randomly and independently sampled from their population. Extreme outliers were identified and excluded from data analysis.

3. Results

3.1. As(III) and As(V) comparative toxicity in T. thermophila strains

As(III) or As(V) cytotoxical analyses from cellular populations of the five different *T. thermophila* selected strains; SB1969, GFPMTT1, GFPMTT5, MTT1KO and MTT5KD, were carried out. Comparison of acute toxicity between As(III) and As(V) was made, using as endpoint the median lethal concentration (LC_{50}). These results are shown in the Table 1, which also reports the LC_{10} and LC_{90} values for As(III) or As(V), in SB1969, GFPMTT1 and GFPMTT5 strains.

In the *T. thermophila* wild type strain the LC_{50} values are 180 μM for As(III) and 75 μM for As(V) (Table 1); therefore arsenate is almost 2.5 times more toxic than arsenite. This toxicological situation changes drastically in genetically modified strains (GFPMTT1 and GFPMTT5) which have many more copies of each MT (MTT1 or MTT5). LC_{50} values for the GFPMTT1 strain are 575 μM for As(III) and 1278 μM for As(V) (Table 1), arsenite being about 2.2 times more toxic than arsenate.

Similar results are shown by the GFPMTT5 strain, the LC_{50} value for As(III) is 527 μM, while for As(V), it is 1238 μM, arsenite is about 2,3 times more toxic than arsenate. Both strains are more resistant to As(III) or As(V) than wild type strain, since As(III) or As(V) concentrations to reach 50% mortality are higher than in the wild-type strain. However, a switch from the higher toxicity of arsenate (as sowed in the wild strain) to that of arsenite is detected: in these strains arsenite is more toxic than arsenate. Something similar is obtained for the LC_{90} values (Table 1), but not for the LC_{10} values where it is maintained that arsenate is more toxic than arsenite. At the lowest As(III) or As(V) concentrations and cell mortality (LC_{10}) the same toxicity pattern is maintained: As(V) is more toxic than As(III) in all three strains (Table 1), with values of 15.6x (SB1969), 8.3x (GFPMTT1) and 7.5x (GFPMTT5). But in GFPMTT1 and GFPMTT5 strains the toxicity pattern is reversed [As(III) > As(V)] as the concentrations of both metalloids and mortality percentages are increased (Table 1): 2.2x (GFPMTT1) and 2.3x (GFPMTT5) for LC_{50} or 5.1x (GFPMTT1) and 5.2x (GFPMTT5) for LC_{90} concentration.

With regard to the MTT1KO and MTT5KD strains their LC_{50} values show that the tolerance to As(III) or As(V) is significantly lower than that in the wild type strain (Table 1). The total or partial deletion of the genes encoding metallothioneins (MTT1 or MTT5) strongly affected arsenic tolerance in both strains, but the results differ depending on which MT gene has been totally or partially eliminated (Table 1). In the both strains, As(III) and As(V) cause high cell mortality at low concentrations compared to the wild-type, and likewise the toxicities of both metalloids are reversed with respect to the control strain; As(III) is more toxic than As(V), at least in strain MTT1KO, while in MTT5KD the toxicities of both are more similar (Table 1). The selective toxicity coefficients, calculated as LC_{50} (A) / LC_{50} (B) and viceversa, between strains GFPMTT1 and GFPMTT5 show that both have similar resistance levels to As(III) and As(V). On the other hand, strain MTT1KO is more resistant to As(V) than strain MTT5KD, and the latter is more resistant to As(III) than strain MTT1KO.

Dynamics of dose-effect curves, adapted to a logistic model, for each arsenic compound [As(III) or As(V)] in the SB1969 wild-type strain are reported in Fig. S1.

Table 1
As(III) or As(V) LC_{50}, LC_{10} and LC_{90} values (at μM concentration), calculated from their dosage-mortality Probit model, for *T. thermophila* SB1969, GFPMTT1, GFPMT5, MTT1KO and MTT5KD strains (confidence interval 95%). ND: not determined.

Strain	Treatment	LC_{50}	LC_{10}	LC_{90}
SB1969	As(III)	180	47	313
	As(V)	75	3	147
GFPMTT1	As(III)	575	318	833
	As(V)	1278	38	4270
GFPMTT5	As(III)	527	271	784
	As(V)	1238	36	4144
MTT1KO	As(III)	8	ND	ND
	As(V)	35	ND	ND
MTT5KD	As(III)	20	ND	ND
	As(V)	22	ND	ND

3.2. Toxicity evaluation of binary mixtures in the wild-type strain

As previously indicated, the *T. thermophila* toxicity to As(III) or As(V) are markedly different. Considering that both forms of arsenic may be present in the same environment, we have analyzed the joint toxicities of binary mixtures of As(III) and As(V) in the wild-type strain of this microorganism, in order to detect possible synergisms. For this purpose, we have applied the Concentration Addition model, which have been often used as a traditional model to evalue the metal mixture toxicity. Table S3 shows results of the different combinations and relative tested concentrations of As(III) and As(V), as well as their standard errors and p-values from the ANOVA test ($\alpha = 0.05$). All statistical analyses (ANOVA) were carried out for each block of As(III) and As(V) combinations with the same final TU, with a p-value > 0.05 (Table S3). Results indicate that there is no significant difference between the toxicities of mixtures and individual As(III) or As(V) treatments at different concentrations (Table S3). Therefore, we conclude that there is no synergism between As(III) and As(V), regardless of the concentrations used of each arsenic ionic form in the mixtures, there being an additive effect.

3.3. ROS generation and mitochondrial membrane potential assessments

Superoxide anions are both important oxidative stress inducers and

responsible to produce other ROS/RNS species such as H_2O_2 and $ONOO^-$ (peroxinitrile). When *T. thermophila* SB1969 populations are exposed to low concentrations of As(III) or As(V) (5 μM), there are no significant differences with respect to the control sample, after testing with the HE fluorochrome (5 μg/mL final concentration, 30 min treatment) (Fig. 1). However, when As(III) or As(V) concentrations are higher, increasing levels of HE fluorescence are detected (Fig. 1, Table S4). Regardless of the different lethality levels of As(III) or As(V) in this ciliate (Table 1), the overall production of reactive species (superoxide, H_2O_2 and peroxynitrile, mainly) is similar under the same concentration from each arsenic ionic form (Fig. 1).

To confirm this statistically, a logarithmic model including a dose-treatment interaction parameter was carried out. This model confirms that, increasing As(III) or As(V) concentrations result in higher levels of peroxide ions and secondarily the ROS/RNS values (p-value < 0.0001). The p-value for this interaction parameter is > 0.05 (0.324), which means that using As(III) or As(V) is indifferent, since similar levels of toxic ions are produced. Therefore, the differences between the lethality levels for As(III) and As(V) cannot be explained exclusively on the basis of the production of these ions.

Likewise, intracellular levels of hydrogen peroxide, peroxynitrite, nitric oxide and some other monoeletronic oxidants were assessed in the wild-type of ciliate after As(III) or As(V) treatments by using the non-fluorescent molecule DHR123. The oxidized form of DHR123 (rhodamine 123) fluoresces, and thus ROS/RNS is detected in mitochondria. Results in Fig. 2 show that, there is no significant difference in the fluorescent emission of oxidized DHR123 at low As(III) concentrations (5–25 μM) with respect to the control, and at concentrations above 25 μM the fluorescent emission continues decreasing significantly with respect to the control. Therefore, either As(III) causes intense mitochondrial damage or it does not generate these free radicals.

In contrast, As(V) at 5–25 μM concentrations generates fluorescent emission that is about 40 times higher than the control (Fig. 2). But from an As(V) concentration 50 μM and higher, a gradual decrease in fluorescence emission is detected (Fig. 2, Table S5).

As was previously done, to test this a predictive model was developed with the experimental data. In this logarithmic model all considered parameters showed statistical significance, including the treatment-dose parameter added to prove the probable interaction between both variables (p-value $= 0.009$). This is sufficient statistical evidence to infer that, at low concentrations As(V) generates higher levels of H_2O_2, $ONOO^-$ and other monoelectrononic oxidants than As(III) at the same concentrations or the control. Starting at 50 μM for both As(III) or As(V), there is a significant reduction in the production of these toxic ions, attributable to a reduction in the number of viable cells as the LC_{50} value of As(V) or the LC_{10} of As(III) is reached (Table 1). Additionally, these data could corroborate, at least partially, the higher toxicity of As(V) at low concentrations, with respect to As(III) (Table 1).

To study the comparative effect of As(III) and As(V) on mitochondrial membrane potential ($\Delta\psi_{mt}$), populations of *T. thermophila* were exposed (during 24 h) to the following increasing concentrations 10, 25, 50, 100, 200 and 400 μM of each of them, and treated with the fluorochrome JC-1. As shown in Fig. 3 and Table S6, both As(III) and As(V) cause a gradual loss of mitochondrial membrane potential. This depolarization of the mitochondrial membrane is intensified from 50 μM As (III) or As(V), decreasing the relative fluorescent ratio (FR) by about 60% and reaching a 70% decrease at 400 μM (Fig. 3).

To know the existence of significant differences between As(III) or As (V) treatments, as well as between treated samples and controls, an ANOVA was carried out with doses and treatments as independent variables. Dose was a significant variable (p-value ≤ 0.0001) while treatment was not (p-value $= 0.4338$), confirming that arsenic dose, regardless of whether it is As(III) or As(V), generates a change in mitochondrial membrane potential.

A Least Significant Difference (LSD) multiple comparison procedure was applied to analyze the differences between fluorescence quotients for the different doses (Table S7). The LSD method identified 5 homogeneous groups of data: the first includes the positive control data, the second includes the 10 and 25 μM concentrations, the next the data corresponding only to 50 μM, the fourth 100, 200 and 400 μM concentrations and a final group including the negative control (Table S7). This analysis confirms that increasing arsenic concentration, regardless of whether it is As(III) or As(V), causes a statistically significant reduction in mitochondrial membrane potential, only dependent on concentration used for each arsenic ionic form. Therefore, concentrations of 10 and 25 μM cause the same loss of membrane potential (about 10%). In the next group (50 μM concentration) causes a loss of membrane potential of more than 50%. Finally, a third group, including 100, 200 and 400 μM concentrations cause the same loss of mitochondrial membrane potential (about 70–75%). These three groups are significantly different from the other two control groups (positive and negative) (Table S7).

3.4. Ultrastructural analysis of As(III) or As(V) treated cells

Fig. 4 (A and B) illustrates the general appearance of a *T. thermophila* cell and its macronucleus (Ma), respectively. Cells treated (2 h) with As

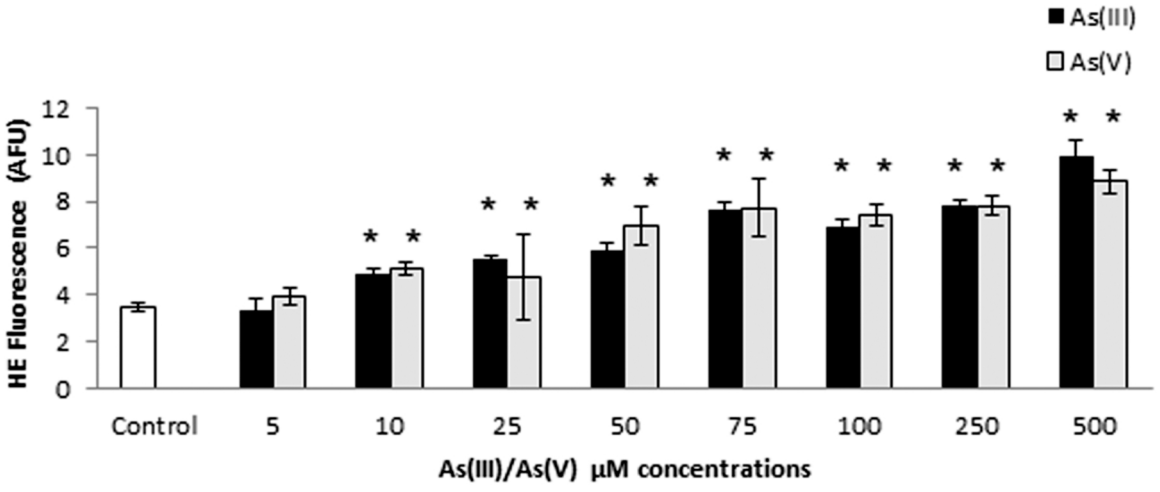

Fig. 1. Comparative HE mean fluorescence emission values from *T. thermophila* SB1969 populations exposed to increasing concentrations (μM) of As(III) or As(V) for 24 h ($n = 4$). Negative controls were included in every assay. AFU: arbitrary fluorescence units. One-way ANOVA tests asterisks indicate significant differences between As(III) or As(V) treatments and the control sample ($p < 0.05$).

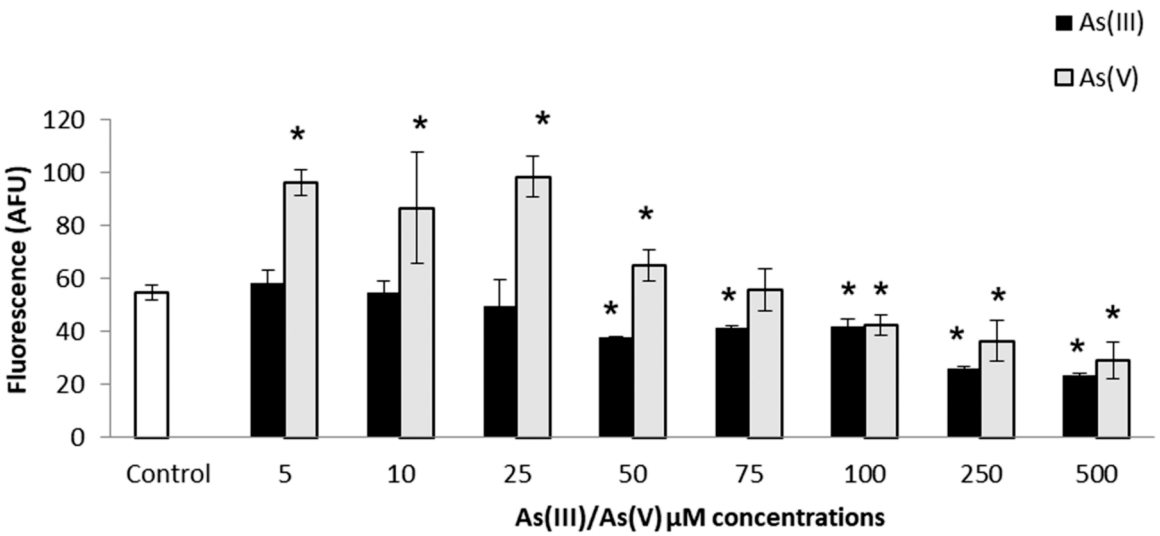

Fig. 2. Comparative DHR123 mean fluorescence emission values from *T. thermophila* SB1969 populations exposed to increasing concentrations (µM) of As(III) or As (V) for 24 h (n = 3). Negative controls were included in every assay. AFU: arbitrary fluorescence units. One-way ANOVA tests asterisks indicate significant differences between As(III) or As(V) treatments and the control ($p < 0.05$).

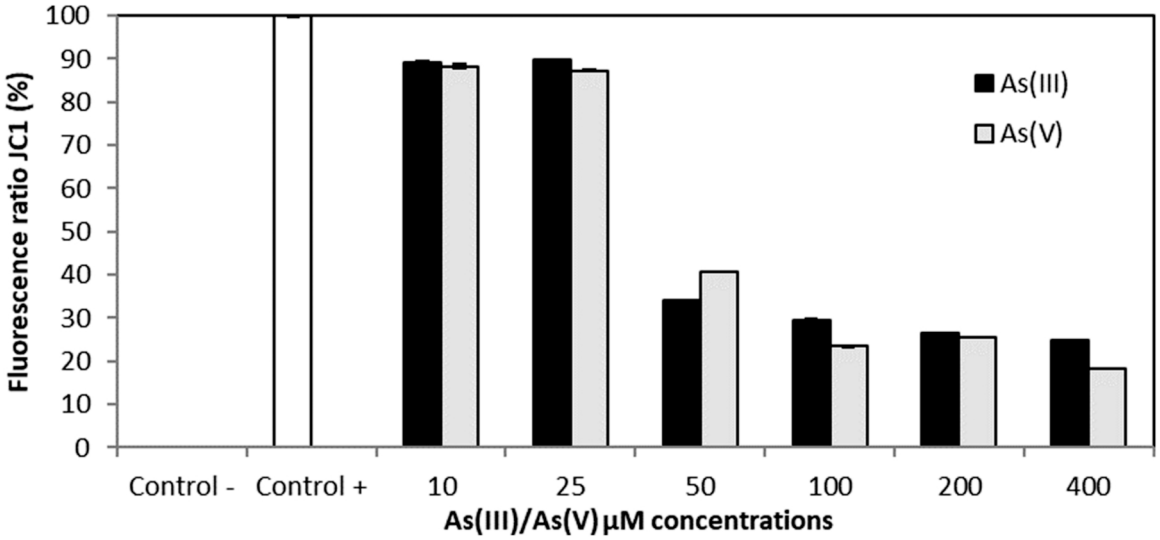

Fig. 3. Fluorescence ratio values from *T. thermophila* SB1969 populations exposed to increasing concentrations (µM) of As(III) or As(V) for 24 h (n = 3), and treated with JC-1 fluorochrome (n = 3). Positive (untreated sample, relative fluorescence ratios 100%) and negative (cells treated with the respiratory uncoupler CCCP, relative fluorescence 0%) controls were included in every assay. In Table S7 the clustering of JC-1 fluorescence quotient means into 5 groups according to whether they are significantly equal to each other is reported.

(V) at 30 µM (concentration generating about 30% lethality) are shown in Fig. 4C-E. The presence of numerous vacuoles, with electrolucent content and numerous membranous structures, together with autophagosomes and specially autophagolysosomes in different grades of degradation, can be observed in Fig. 4 C. Both, an autophagolysosome carrying a degrading mitochondrion (Fig. 4D) and a vacuole with numerous residual membranes (Fig. 4E) can be detected in cells exposed to As(V). In addition to macroautophagy, in cells treated with As(V) for 24 h, three processes involving mitochondrial damage or degradation can be detected, such as mitochondrial fusion (Fig. 4 F, 5 C), mitophagy (Fig. 5 A,B) and mitochondrial swelling (Fig. 4 F, 5 C, D). As a consequence of mitochondrial swelling, electrolucent vesicles appear in these cells, the content of which is expelled out of the cell (Fig. 4 F, 5 C, D).

Regarding the macronuclear system, two main alterations can be observed; a greater number of condensed regions of macronuclear chromatin, and more condensed and a greater number of nucleoli (Fig. 5E). The micronucleus appears far away from the macronuclear pocket, and is more or less spherical in shape (Fig. 5E). As(V) induces mucocyst biogenesis, which are subsequently discharged, releasing their glycoprotein content (Fig. 4F, 5F).

As(III)-treated cells (24 h) show intense lipophagy: a progressive increase of lipid droplets that fuse together, occupying a large region of the cell (Fig. 6 A,D). Likewise, mitochondrial clusters are detected that lead to degradation of these organelles (Fig. 6A, C). At the macronuclear level, an intense chromatin disorganization (decondensation) and nucleolar fusion are detected (Fig. 6B). No mitophagy signals are detected in As(III)-treated cells.

3.5. *Differential gene expression of selected antioxidant genes*

For RT-PCR analysis, we selected seven genes encoding antioxidant enzymes or MTs: two omega (O) class glutathione-S-transferases (GST)

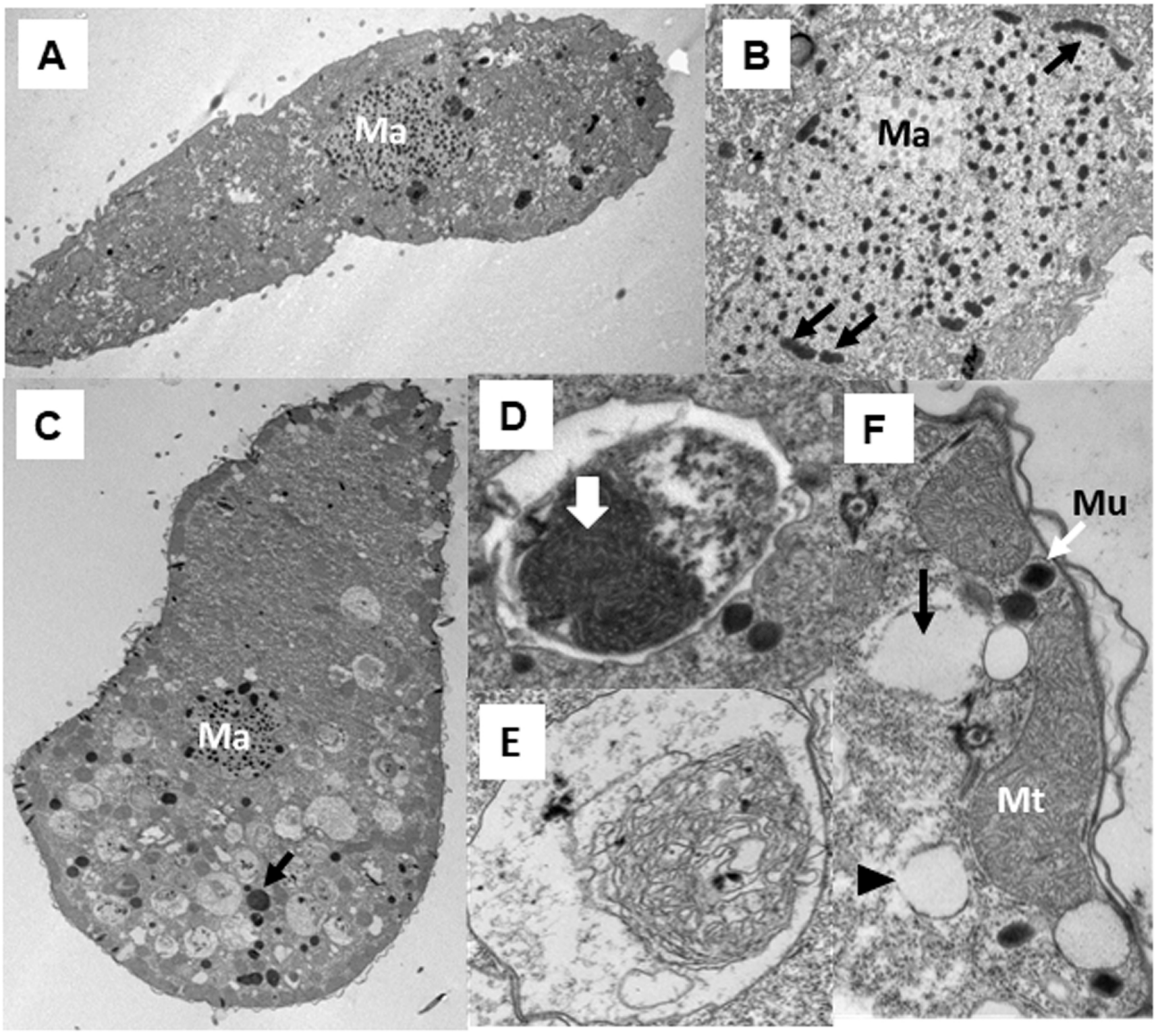

Fig. 4. Ultrastructural images of *T. thermophila*. (A-B): Control sample. A: General appearance of a cell (4Kx). B: Macronucleus (Ma), showing the chromatin organization and peripheral nucleoli (black arrows) (8Kx). (C-E). Cells exposed to As(V) (2 h). C: Section of a cell with an intense vacuolization and autophagolysosomes (black arrow) (4Kx). D: Detail of an autophagolysosome. Degradation of a mitochondrion (dark region) (with arrow) is observed (12Kx). E: Remnants of membranes inside a vacuole (12Kx). F: Cells expoxed to As(V) (24 h). Mitocondrial swelling (black arrow) can be observed. Mucocysts (Mu) (white arrow). Arrowhead indicates membrane rupture. (25Kx).

(GSTO1 and GSTO6), glutathione reductase 1 (GR1), two thioredoxin reductases (TR2 and TR5), and two metallothioneins (MTT1 and MTT5) from the genome of *T. thermophila*. Table S8 and Fig. 7 show the relative fold induction expression values of these selected genes from cell samples treated (1 or 24 h) under As(III) or As(V) (10 μM).

The two selected omega class GST genes (TtGSTO1 and TtGSTO6) exhibit quite similar induction patterns. They show certain induction (about 4-fold) at 1 h As(III) treatment while at 24 h the induction is considerably reduced. The induction values under As(V) stress are quite similar at different exposure times, although somewhat higher in the TtGSTO6 gene (Fig. 7, Table S8). The only GR gene present in the genome of *T. thermophila* is not induced under As(III) stress, but its expression is very strongly induced in the presence of As(V) (about 294-fold after 24 h treatment) (Fig. 7, Table S8).

The two selected TR genes show very different gene expression induction patterns against As(III) or As(V). The *TtTR2* gene is not induced by As(III) at 1 h of treatment, whereas it is significantly (32-fold) induced after 24 h As(III) treatment. The opposite occurs for the *TtTR5* gene, which is induced by As(III) after 1 h of treatment (about 4-fold), and is not induced after 24 h of treatment. Both genes are induced by As(V), although more strongly after 1 h than at 24 h of treatment (Fig. 7, Table S8). Finally, the two MT genes (*MTT1* and *MTT5*) respond differently to As(III) or As(V), although the *MTT5* gene is induced more than *MTT1* under all conditions tested (Fig. 7, Table S8). A comparative analysis among all analyzed genes shows the following ranking of expression induction values under As(III) or As(V) stress: As(III)− 1 h: *TtMTT5* > *TtTR5* > *TtGSTO1* > *TtGSTO6*; As(III)− 24 h: *TtTR2* >> *TtMTT5* > *TtMTT1*; As(V)− 1 h: *TtTR5* > *TtTR2* >> *TtGR1* > *TtGSTO6* > *TtGSTO1* > *TtMTT5*; As(V)− 24 h: *TtGR1* >> *TtTR5* > *TtMTT5* > *TtMTT1* > *TtTR2* = *TtGSTO1* = *TtGSTO6*.

4. Discussion

4.1. Comparative cytotoxicity of arsenite and arsenate and their binary mixtures

There are many published scientific works on the toxic effects of As (III) and/or As(V) on many different organisms, both unicellular and multicellular, eukaryotic and prokaryotic (Bali and Sidhu, 2021; Byeon et al., 2021; Miazek et al., 2015; Ozturk et al., 2021). However, there are very few studies comparing the toxicity of both ionic forms in the same organism. In addition, there is a great diversity of methodologies and parameters to evaluate the toxicity of this metalloid among the different authors, which makes it difficult to carry out a correct comparative

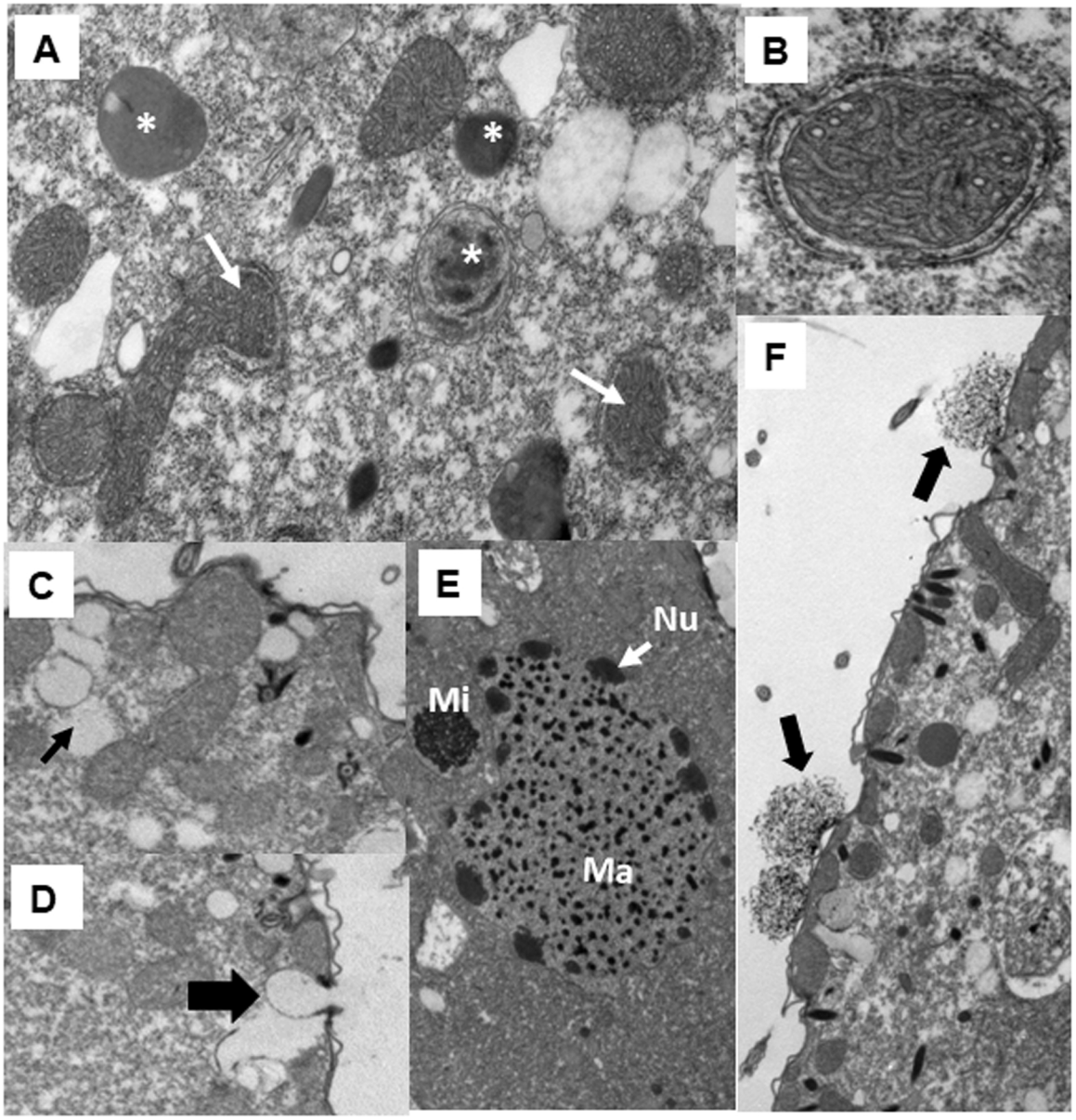

Fig. 5. (A-F): Ultrastructural images of *T. thermophila* exposed to As(V) (24 h). A: Cytoplasm showing different stages of an intense mitophagy process (8Kx). Asterisks: late mitophagolysosomes. White arrows: mitophagosomes. B: A mitophagosome in formation (50Kx). C: Long mitochondrion and mitochondrial swelling (black arrow) (8Kx). D: Electrolucent vesicle, derived from mitochondrial swelling, spilling its content out of the cell (black arrow) (6Kx). E: Macronucleus (Ma) and Micronucleus (Mi). Nu= Nucleolus (white arrow). F: Mucocyst discharge (black arrows) (6Kx).

analysis. The few available quantitative studies about As(III) and/or As (V) cytotoxicity stated that arsenite is more toxic than arsenate in aquatic animals, mammals (including human cells lines) and plants (Byeon et al., 2021; Coelho et al., 2020; Stýblo et al., 2021). However, it must be pointed out that each species, and even each strain, presents a specific quantitative-qualitative response against these different arsenic inorganic forms, together with a different set of different resistance mechanisms for each of them.

There are two previous works on arsenic toxicity in *Tetrahymena* species; one is in *T. pyriformis* assessing the GI_{50} (growth inhibition) parameter at 40 μM As(V) after 18 h of treatment (Zhang et al., 2012), and the second is in *T. thermophila* with average CI_{50} (concentration inhibition) values (36 h of treatment) for As(III) and As(V) of 1.62 and 1.96 mg/L, respectively (Zhang et al., 2015). Our results on *T. thermophila* (strain SB1969) show that As(V) (with an $LC_{50} = 75$ μM or 10.5 mg/L) is about 2.5 times more toxic than As(III) ($LC_{50} = 180$ μM or 19.3 mg/L), after 24 h treatment. From which it can be inferred that in this *T. thermophila* strain As(V) is more toxic than As(III), and these results differ considerably from those shown by Zhang et al. (2015). These differences could be due to several reasons: 1- the different methodologies used to assess toxicity; the colorimetric MTT assay (Zhang et al., 2015) or flow cytometry (this research work), 2- the endpoint to evaluate cellular toxicity; inhibition concentration parameter used by Zhang et al. (2015) or the median lethal concentration parameter used by us), 3- the exposure time; 36 h (Zhang et al., 2015) or 24 h in our study, and 4- the composition of the medium in which the toxicity test was performed; a rich growth medium (Zhang etal, 2015) or TrisHCl buffer in this work. Due to all these differences, we cannot consider both assays comparable even if they were carried out with the same microorganism.

As in *T. thermophila*, there are other microorganisms (prokaryotes and eukaryotes) in which As(V) is more toxic than As(III). This occurs in several species of freshwater and especially marine microalgae, such as *Stichococcus bacillaris* (Pawlik-Skowronska et al., 2004), *Chlorella salina* (Karadjova et al., 2008), *Monoraphidium arcuatum* (Levy et al., 2005)

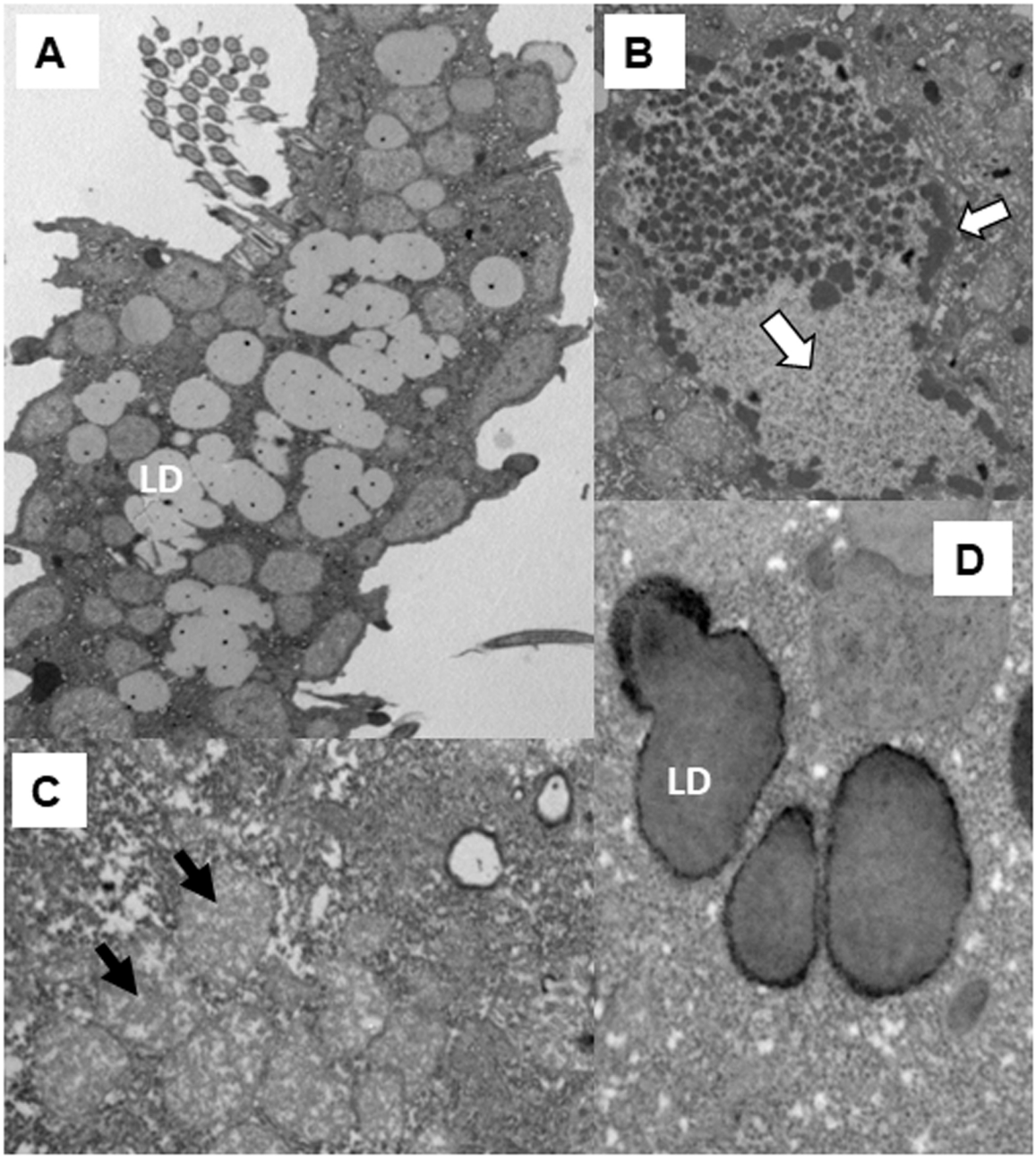

Fig. 6. A-D: Cells exposed to As(III) (24 h). A: Longitudinal section of an arsenite treated cell. A severe lipophagy and mitochondrial clusters are detected (8Kx). **B:** Macronuclear chromatin disorganization and nucleolar fusion (white arrows) (12Kx). C: Mitochondrial cluster degradation (black arrows) (25Kx). D: Mature lipid droplets (LD) (5Kx).

and *Chlorella* sp. CE-35 (Rahman et al., 2014). It also occurs in certain bacteria, for instance *Acidithiobacillus caldus* (Kotze et al., 2006) and *Vibrio parahaemolyticus* (Shakya et al., 2012).

The levels of resistance of *T. thermophila* (SB1969) to As(V) are higher than those reported in other microorganisms: the ciliate *T. pyriformis* (IC_{50} = 40 μM) (Zhang et al., 2012), the microalgae *Scenedesmus obliquus*, and *Ankistrodesmus falcatus* and several groups of aquatic invertebrates, such as the marine rotifer *Brachionus plicatilis* (Byeon et al., 2020), the cladocerans *Ceriodaphnia* cf. *dubia* (Rahman et al., 2014) and at least three species in the genus *Daphnia* (He et al., 2009; Shaw et al., 2007; Wang et al., 2018). Likewise, other invertebrates (copepodes and crustaceans) used in different bioassays, showed more tolerance to As(V) (Byeon et al., 2020; Gutu et al., 2015). In addition, *T. thermophila* (SB1969) resists higher levels of As (III) than those found in aquatic microinvertebrates (rotifers, cladocerans and copepods) (Byeon et al., 2021), and some microalgae (Levy et al., 2005; Zhang et al., 2013b). The most As(III)-resistant microalgae reported so far is the polyextremophilic *Chlamydomonas acidophila* RT46 (LC_{50} = 10.91 mM or 817.7 mg/L), isolated from Tinto River, an acid aquatic ecosystem which contain high concentrations of several metal(loid)s (incuding arsenic) (Diaz et al., 2020). In general, both Gram-positive and -negative bacteria are much more resistance to As(III) than euharyotic microorganisms (LC_{50} values are included in the range 10–300 mM) (Nagvenkar and Ramaiah, 2010; Ordoñez et al., 2005).

Many experts agree that metal(loid) contamination in both aquatic and terrestrial ecosystems is usually multiple, and rarely a single metal (loid) is present (He at al, 2009). Likewise, it is well known that in the case of arsenic pollution, As(III), As(V) and smaller amounts of

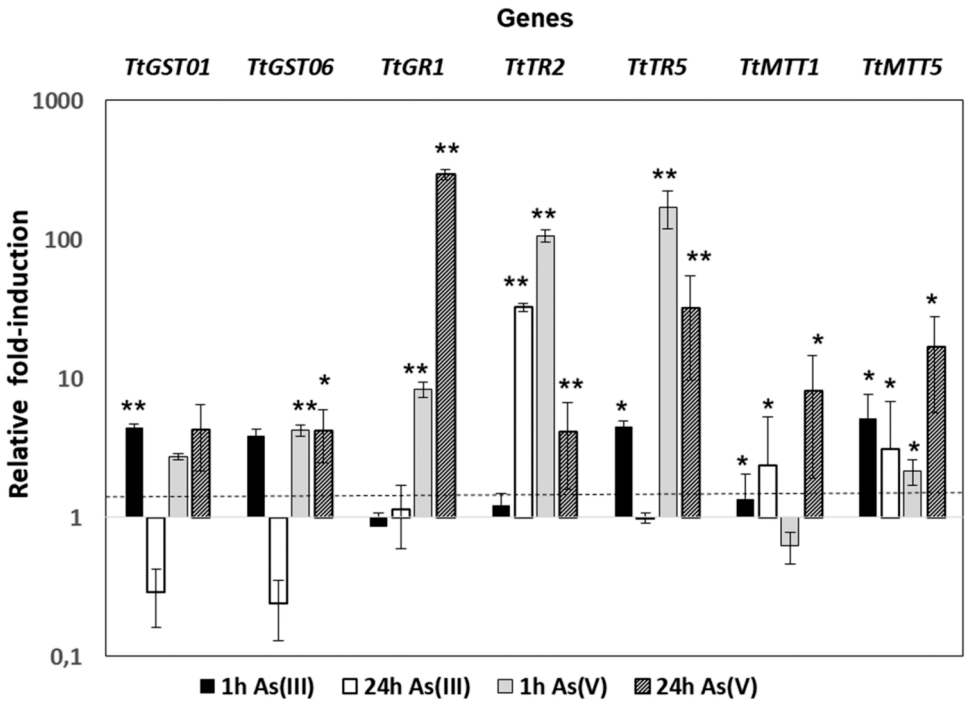

Fig. 7. Relative fold induction expression values of the seven selected genes under As(III) or As(V) (10 μM) 1 or 24 h treatments. Expression induction is considered positive when the fold induction value obtained is > 2 (indicated by the dashed line). One or double asterisk indicates significant differences at $p < 0.1$ or $p < 0.05$, respectively.

organoarsenical compounds coexist in aquatic ecosystems (Al-Makishah et al., 2020; Shaji et al., 2021; Sharma and Sohn, 2009). So it seems paradoxical that in many countries water quality guidelines evaluate the total amount of arsenic, rather than the different arsenic species present in the water ((WHO), 2011). Studies about binary metal mixtures toxicities have focused mainly on arsenite and its interaction with essential (Cu, Cr) (Eze et al., 2019; Kilpi-Koski et al., 2020) and non-essential metals (Cd, Hg, Pb) (Eze et al., 2019; Karri et al., 2018; Vellinger et al., 2012; Yoo et al., 2021). Furthermore, it is interesting to note that the type of interaction in the As(III)-Pb(II) mixture depends on the cell type used in the bioassay. The As(III)-Pb(II) interaction is additive in two mammalian cell lines (Karri et al., 2018; Eze et al., 2019), while in the brackish water flea *Diaphanosoma celebensis* it is synergistic (Yoo et al., 2021).

As far as we know, there is only one published paper about the interaction arsenite-arsenate in binary mixtures, using the planktonic crustacean *Daphnia carinata* as testing organism (He et al., 2009). This study indicates that As(III) and As(V) can interact additively, but this interaction changes to the synergistic type when the bioassay is carried out in river water (He et al., 2009). In all bioassays realized on *T. thermophila* the results have shown an additive effect between As(III) and As(V), regardless of the concentrations used for each form of arsenic. According to a recent exhaustive meta-analysis (Martin et al., 2021), an additive effect is the most frequent result obtained from binary chemical mixtures. Additive effect has also been considered as a non-interaction event, and the possible mechanisms involved are still unknown (Walker et al., 2012).

4.2. ROS generation and mitochondrial membrane depolarisation

As is well known, one of the main mechanisms of As(III) and arsenic trioxide toxicity is the production of ROS and/or RNS in living beings. However, data on the toxicity of As(V) are scarce and unclear (Abbas et al., 2018; Byeon et al., 2021; Hu et al., 2020; Jomova and Valko, 2011; Nurchi et, 2020). In both human and other mammalian cell lines, it has been shown that arsenic inorganic forms can generate two main types of oxidizing molecules; superoxide anion ($O_2^{\cdot-}$) and hydrogen peroxide (H_2O_2), and from them, other ROS and RNS can be generated, such as hydroxyl ions (OH^-), hydroperoxyl radicals ($HOO^{\cdot}$), singlet oxygen ($^1O_2$), peroxyl radicals ($ROO^{\cdot}$) and peroxynitrite ($ONOOH$) (Flora et al., 2007; Hu et al., 2020; Shi et al., 2004; Valko et al., 2016; Winterbourn et al., 2004). In aerobic microorganisms, few quantities of intracellular oxygen free radicals and hidrogen peroxide are originated by certain enzymatic activities and, specially, in the mitochondrial electron transport chain, which are blocked by diverse antioxidant molecules (Phaniendra et al., 2015), or they can be involved in redox signaling (Sies and Jones, 2020). However, the presence of arsenic generates large amounts of ROS/RNS, which can no longer be neutralized by the antioxidant defense.

In *T. thermophila*, both As(III) and As(V) treatments (5–500 μM, during 24 h) cause a similar increase in the superoxide and/or peroxynitrite ions production, with respect to the levels of control samples. Formation of superoxide radicals, after exposure to arsenic, has been reported in some human, animal and microalgae cell lines (Diaz et al., 2020; Fan et al., 2015; Guidarelli et al., 2019; Lynn et al., 2000). Using the DHR123 assay, we have detected in *T. thermophila*, that As(V) originates more H_2O_2 and peroxinitrite than As(III), under the same concentrations and exposure time, indicating a higher mitochondrial damage. Within the sub-lethal concentration range (5–50 μM), As(V) causes higher levels of hydrogen peroxide and peroxynitrite than As(III) in the same concentration range. This could explain the greater toxicity of As(V) with respect to As(III) in *T. thermophila*, since both produce the same levels of superoxide anion, but As(V) also causes greater increases in hydrogen peroxide and peroxynitrite. Likewise, this corroborates results indicating that arsenic causes mitochondrial dysfunction. The adverse effects of arsenic on mitochondria, including membrane depolarization, have been widely reported (Blajszczak and Bonini, 2017; Prakash et al., 2016, 2021).

4.3. Differential ultrastructural alterations by arsenic stress

It is widely known that mitochondria are crucial organelles involved

in many relevant cellular functions, such as redox celular signaling, calcium homeostasis, energy production, fatty acid metabolism and cell death. As previously indicated, mitochondria are one of the most important targets of the adverse effects of arsenic, and, as also detected in *T. thermophila*, this metalloid induces mitochondrial dysfunction. The main ultrastructural manifestations of these adverse effects of arsenic on mitochondria from the ciliate *T. thermophila* are described in the following paragraphs. Longer mitochondria have been observed in cells treated with As(V) for 2 or 24 h, whereas As(III) does not produce this effect. In addition, As(V) causes an intense process of selective mitochondrial autophagy (mitophagy), as well as a rather great process of mitocondrial swelling. Therefore, mitochondria damaged by As(V) treatment can be degraded either by a non-selective autophagy process or by mitophagy (a mitochondrial autophagy selective mechanism) (Kotiadis et al., 2014). Mitochondrial swelling also appears in As (III) treated cells, but in this case, mitochondrial cristae alterations and membrane rupture are the main ultrastructural signs of mitocondrial degradation. Ultrastructural images of these arsenite damaged mitochondria remember the morphological hallmarks of a type of cell programmed death process iron-dependent and characterized by a lipid peroxidation, known as ferroptosis (Lei et al., 2019; Li et al., 2020; Meng et al., 2020). Ferroptosis induction by arsenite has been observed in certain mammlian cell lines (Wei et al., 2020). In *T. thermophila*, both arsenic inorganic forms cause intense structural alterations, although the effects observed in cells treated with As(V) are not completely identical to those caused by As(III). Mitochondrial alterations induced by metal(loid) exposure have been described in several ciliate species (Martin-Gonzalez et al., 2005; Piccinni et al., 1987). Specific mitochondrial ultrastructural alterations (extensive swelling and matix rarification) have been reported in mammalian cells and chickens, after As (V) (Fei et al., 2019, 2020), As(III) (Fowler et al., 1977) or arsenic trioxide treatments (Wang et al., 2018). The existence of mitophagy to remove irreversibly damaged mitochodria has been detected in mice (Zeinvand-Lorestani et al., 2018) and *Caenorhabditis elegans* (Luz et al., 2017) after As(III) exposure.

The presence of numerous autophagosomes and autolysosomes, indicating an intense autophagy, in *T. thermophila* exposed to As(V) during 2 h reveals the high cytotoxicity of this compound. Autophagy (macroautophagy) is a common eukaryotic homeostatic mechanism; in fact, almost all cell types have basal levels of autophagy, but is considerably increased under environmental stress, in special by toxic chemical agents generating ROS (Garza-Lombó et al., 2020). In many cases, stress-induced autophagy acts as a pro-survival mechanism, but this process can also lead to cell death. (Doherty and Baehrecke, 2018). Induction of autophagy has been profusely described in cells treated with different inorganic forms of arsenic and other metal(loid)s, and in some cases jointly induced apoptosis has been detected. (Chiarelli and Roccheri, 2012; Chatterjee et al., 2014; Fu et al., 2021; Wu et al., 2021). Other inducers of an autophagic process reported in *Tetrahymena* species and other ciliates are the herbicide paraquat (Diaz et al., 2016) and cadmium (Martin-Gonzalez et al., 2005).

The presence of intense cytoplasmic vacuolization caused by exposure to As(V) is not only detected in *T. thermophila*, but also in other cell types or microorganisms, such as: rat hepatic cells (Muthumani and Miltonprabu, 2015), tilapia cells (Ahmed et al., 2013), the microalgae *Scenedesmus quadricauda* (Zhang et al., 2013a) and *Chlamydomonas acidophila* (Diaz et al., 2020).

Some protists have organelles (extrusomes) that, under certain stress conditions, can extrude or discharge their contents (protein or glycoprotein) out of the cell (Kaur et al., 2017; Rosati and Modeo, 2003). The ciliate *T. thermophila* have large secretory extrusomes known as mucocysts (Rosati and Modeo, 2003). As(V) induces mucocystic extrusion in *T. thermophila*, as observed by electron microscopy (Fig. 5 F). Likewise, in this same ciliate, a mucocystic extrusion process has been observed after treatment with other metal(loid)s or metallic nanoparticles (unpublished data). This mucocystic extrusion could be interpreted as an additional barrier to minimize exposure to various environmental toxic pollutants.

An interesting finding is the detection of numerous lipid droplets in the cytoplasm of *T. thermophila* after exposure to As(III), which may subsequently undergo lipophagy. For a long time, lipid droplets (LDs) have been only considered as lipid reservoirs, but they are now recognized as true organelles, which follow different phases, such as biogenesis, maturation, interaction with other organelles and degradation (Cohen, 2018). The observation of intracellular accumulation of LDs in response to As(III) is not new, although its true significance is not yet clarified (Fowler et al., 1977; Muthumani and Miltonprabu, 2015). In mammals, arsenic exposure originates a lipid metabolism dysfunction, but these results are not conclusive (Zhao et al., 2020). Other authors consider As(III) and other toxic metal(oid)s to be a potential obesogen (chemical compounds that can supposedly to disrupt normal development and balance of lipid metabolism or an adipotropic effect, which in some cases, can lead to obesity) (Tinkov et al., 2021). In human cells, numerous LDs assemble around the nucleus immediately before the ferroptosis process occurs (Meng et al., 2020). In the microalga *Nannochoropsis* sp. the lipid intracelular content decreases under arsenic trioxide treatment (Sun et al., 2015). According to electron microscopy images from *T.* thermophila exposed to As(III) (Fig. 6A, D), an abnormal extreme lipid accumulation is detected in these cells, which may indicate lipogenesis or a lipid metabolism dysregulation. A relevant proportion of these new formed LDs are removed by lipophagy (Schott et al., 2019). Unfortunately, there is currently no published work on the possible links between environmental pollution and lipid metabolism.

A considerable number of studies both in vivo and in vitro corroborate the genotoxic character of inorganic arsenicals (Jomova et al., 2011; Roy et al., 2018). These arsenic forms cannot interact directly with DNA but can give rise to ROS and/or RNS that could lead genome damage, such as DNA synthesis inhibition or blockage of DNA repair. (Minatel et al., 2018; Muenyi et al., 2015; Tam et al., 2020). In *T. termophila* cells exposed to As(V) two nuclear ultrastructural alterations are detected; more condensed nucleoli or products of nucleolar fusions and separation of the micronucleus from the macronuclear-pocket. Both types of nuclear alterations have been described previously and denote the presence of cellular stress (Gutierrez et al., 1998; Martin-Gonzalez et al., 2005; Piccinni et al., 1987; Romero et al., 2019; Ye et al., 2018). Similarly, under As(III) stress, the macronucleus of this ciliate shows two structural alterations; nucleolar fusion and a macronuclear extensive area with a less condensed or disorganized chromatin. We do not know if these structural alterations are accompanied by specific molecular alterations in the ciliate DNA, or if they constitute general response mechanisms to any environmental stress, since similar alterations induced by other types of stressors (such as starvation or RNA synthesis inhibitors) have been observed in ciliates (Gutierrez et al., 1998).

4.4. Differential transcriptional induction of selected antioxidant genes

As shown, the experimental data corroborate that As(III) or As(V) treatments cause ROS and/or RNS in the ciliate *T. thermophila*. To overcome this toxicity, the cell must increase the intracellular amounts of antioxidant molecules. To elucidate this possibility, a qRT-PCR analysis of selected genes encoding antioxidant proteins or enzymes was carried out. Results show that differential expression values for the same gene depend on the ionic form of arsenic, As(III) or As(V), and on the exposure time (1 or 24 h). In general, it is inferred that As(V) induces higher expression induction values of selected genes, with some exceptions. This corroborates the higher toxicity of As(V) versus As(III) in this ciliate, which, in part, must be counterbalanced by a higher expression of selected genes encoding antioxidant molecules. And depending on the type of selected gene, the induction is higher or lower at 1 or 24 h of treatment.

The glutathione-*S*-transferases (GSTs) are universal enzymes that

catalyze nucleophilic attack by reduced glutathione (GSH) on nonpolar compounds that contain an electrophilic carbon, nitrogen, or sulphur atom (Hayes et al., 2005). Among several functions, GSTs have a detoxification function of products originating from oxidative stress, including those from metal(oid)s. Certain metal(oid)s (As, Cr, Cu, Se, etc.) inhibit the activity of GSTs in humans, animals, and plants, thus inducing the expression of GST genes to overcome this inhibition (Dobritzsch et al., 2020). In the GSH-dependent reduction of methylated-As(V) to methylated-As(III), the role of omega class GSTs has been speculated (Thomas, 2007). However, there is a connection between arsenic resistance and the activity levels of various classes of GSTs. GSH binding to As(III) as well as to methylated-As(III) by a pi class GST (GSTP) to form arsenic triglutathione has been demonstrated in several organisms. The methylated-arsenic triglutathione [$(CH_3)_n$-As(III)$(GS)_3$] complex is subsequently excreted out of the cell by an ABC transporter (Thomas, 2007).

Two species of *Tetrahymena* (*T. pyriformis* and *T. thermophila*) have the ability to biomethylate both As(V) and As(III) (Ye et al., 2014; Yin et al., 2011; Zhang et al., 2012). And with regard to GST family the ciliate *T. thermophila* has 63 isoforms included in four known GST classes; 5 Theta, 2 Zeta, 47 Mu y 7 Omega, plus 2 undetermined (Gutierrez et al., 2008).

The two selected omega class GST paralogs genes from *T. thermophila* used in this study show very similar induction patterns, with induction values not too high (a maximum value of about 4-fold) for both As(III) (1 h) and As(V) (1 or 24 h). An equally moderate overexpression of two different omega GST genes (*GSTΩ1*, *GSTΩ2*) after arsenic exposure has been reported in mollusks (Chen et al., 2018). But, in contrast to what occurs in the ciliate *T. thermophila*, in tissues from clam *Ruditapes philippinarum* the induction values of both GST genes is greater under As(III) stress than with As(V) at low concentrations (Chen et al., 2018). This could also reveal the differences in toxicities of As(III) with respect to As(V) in both organisms, in *T. thermophila* As(V) is more toxic while in mollusks, as in other living beings, As(III) is more toxic. As only two GSTs from the omega class isoforms have been assayed, we cannot confirm the possible function of any omega class GST from this ciliate in the reduction of methyl-As(V) to methyl-As(III), or their possible role in the transfer of GSH to methyl-As(III).

On the other hand, the oxidative methylation ability of methyl-As(III) to methyl-As(V), might be different in *T. thermophila* with regard other organisms. In both *T. pyriformis* (Ye et al., 2014) and *T. thermophila* (Yin et al., 2011) the methylated and dimethylated forms of As(V) predominate over As(III) after 48 h exposure to 40 μM As(V). This could also corroborate the higher toxicity of As(V) with respect to As(III) in *T. thermophila*, since the methylated forms of As(V) and the presence of unmethylated As(III) predominate as the concentration of As(V) in the medium increases (Yin et al., 2011).

A transcriptomic study of arsenic stress in plants (Tripathi et al., 2012) has shown that nine different GST genes are overexpressed in rice while only one GST gene is overexpressed in *Arabidopsis thaliana*. This indicates that there is a wide differential response of GST genes to arsenic stress depending on the type of organism. Pending future analysis of other GST genes from *T. thermophila*, and independently of it, the overexpression of up to 4 times the basal expression of the two selected omega class GST genes indicates the importance of these enzymes in arsenic detoxification of this ciliate.

Glutathione reductase (GR) is responsible for maintaining the supply of reduced glutathione (GSH); one of the most abundant reducing thiols in the majority of cells (Couto et al., 2016). *T. thermophila* has a single gene encoding glutathione reductase (*TtGR1*) (Gutierrez et al., 2008). The expression induction of this gene under As(V) stress is considerably elevated (about 293-fold over the basal level after 24 h of exposure) with respect to As(III), which does not significantly induce the expression of this gene. In fact, it is the most expressed gene under As(V) from all the selected genes. This confirms, again, that As(V) is more toxic than As(III) in this ciliate, and that the main, but not the only mechanism of As(V) detoxification could involve binding to GSH or cession of reducing power to enzymes involved in As(V)-induced ROS depletion. In plants, GR plays an important role in conferring resistance to oxidative stress caused by metal(oid)s (Yousuf et al., 2012). A(V) treatments in rice show increased GR activity (Saha et al., 2017).

In mammalian cells and, probably, in most of eukaryotic unicelular microorganisms as *T. thermophila*, there are two major thiol-dependent antioxidants systems: the thioredoxin (Trx) and the glutathione (GSH). The thioredoxin system comprising NADPH (as a source of reducing power), thioredoxin reductase (TR), and thioredoxin (Trx) which is found to be critical for DNA synthesis and defense against oxidative stress (Lu and Holmgren, 2014). The main substrate of TRs is thioredoxin, which functions as proteins that can yield reducing power to many molecules, including important antioxidant enzymes such as peroxidases (Miller et al., 2018).

The macronuclear genome of *T. thermophila* has 5 TR paralogous genes which belong to the H-TR type (high molecular mass TR), from which the expression of two of them (*TtTR2* and *TtTR5*) have been analyzed in this study. Both genes are significantly and strongly induced under As(V) stress (1 h exposure), and both induction values drop after 24 h treatment, although they are still higher than basal levels. There is also differential expression between the two genes, with *TtTR5* reaching higher induction values than *TtTR2*, regardless of As(V) exposure time.

With respect to As(III) stress, the expression levels of both genes are lower than those induced by As(V), with the exception of *TtTR2* whose expression at 24 h is considerably elevated, reversing the response in the *TtTR5* gene, whose highest expression is at 1 h of treatment. Therefore, there is a differential behavior of both TR genes depending on the exposure time. Again, these results reflect the higher toxicity of As(V) in this eukaryotic microorganism with respect to As(III), since a greater amount of both TRs is required to counteract the toxic action of As(V). There appears to be a coordination in the action of both TR enzymes to respond to As(V) jointly by enhancing the reducing action, and to As(III) temporally by substituting the early action of *TtTR5* for the late action of *TtTR2*.

Studies involving TRs in arsenic toxicity have focused almost exclusively on As(III) and some organic arsenicals using human cell lines. Mainly because As(III) is the most toxic ionic form in mammals and other organisms. In human HHL-5 liver cells, it has been shown (Li et al., 2018) that the levels of transcripts encoding the thioredoxin (Trx1) and thioredoxin reductase (TrxR1) proteins increase after exposure (24 h) to sodium arsenite. Likewise, As(III) can block -SH and -SeH groups (selenoproteins) of antioxidant enzymes, such as GR, TR and Glutathione peroxidases, so that under As(III) stress and to recover the functional levels of these enzymes there should be an overexpression of the genes encoding them (Nurchi et al., 2020; Yao et al., 2015).

Metallothioneins (MTs) are proteins mainly involved in the detoxification of metals, having numerous cysteine residues, and therefore -SH groups, through which to interact with these inorganic contaminants. The ciliate *T. thermophila* has 5 different MTs; 3 of them are preferentially Cd-ZnMTs (TtMTT1, TtMTT3 and TtMTT5) and 2 Cu-MTs (TtMTT2 and TtMTT4). Although they have a higher affinity for these metals, they can bind to other metals (De Francisco et al., 2016; Espart et al., 2015; Gutierrez et al., 2019).

MT gene expression analysis under arsenic stress has been carried out almost exclusively in human and mouse cells, using both As(III) and As(V) (in 9 and 2 papers, respectively) (collected in the review of Rhaman and De Ley, 2017). In practically all the reported cases, an increase in the expression of some MT genes has been detected. Although the study of the molecular interaction between arsenic and the -SH groups from MTs has been carried out exclusively on As(III). Using a recombinant human MT (MT1A), it was found that As(III) binds to the -SH groups from Cys residues with the stoichiometry: $As(III)_6MTCys_{20}$ (Ngu and Stillman, 2006). Likewise, MTs can bind methylated forms of As(III), both monomethylated and dimethylated (Rhaman and De ley, 2017). Thus, it seems to be clear that As(III) and MTs can form stable

complexes, and thus be a possible and additional mechanism of As(III) detoxification. In fact, recombinant human MT1A has been used in the construction of an electrochemical biosensor for detecting As(III) and Hg (II) (Irvine et al., 2017).

With respect to As(V), its possible interaction with MTs has not been analyzed, although it most probably exists too. Therefore, a main function can be attributed to MTs with respect to As(III) toxicity, the immobilization of As(III) ions by forming MT-As(III) complexes and as an indirect consequence of this the reduction of ROS originating from these ions. The function of MTs in response to As(III) or As(V) stress in living beings other than humans (plants, animals or microorganisms) is practically unknown, and much more so in the case of As(V), which, being the least toxic ionic form in many organisms, has been practically forgotten.

Results show that the induction of *TtMTT5* gene expression is the highest under the presence of both As(V) or As(III), and that As(V) treatment (24 h) is that most induces the expression of both genes, corroborating the higher toxicity of As(V) in this ciliate. The importance of the MT function in counteracting the toxic action of As(V) is corroborated in strains GFPMTT1 and GFPMTT5, which have a higher number of copies of each of the MT genes and are more resistant to both As(V) and As(III) (their LC_{50} values are about 16 and 3 times higher than that from the wild type strain, respectively). Both strains show selective toxicity coefficients very similar to each other and close to unity, indicating that both show similar resistance to As(V) and As(III). This is because both plasmid constructs have the same *TtMTT1* gene promoter.

Similarly, strains MTT1KO and MTT5KD show much lower LC_{50} values than the wild type strain (SB1969), indicating that the absence of the *TtMTT1* gene or the *TtMTT5* gene copy number decreases in MTT5KD makes these strains more sensitive to both As(III) and As(V). Furthermore, in strain MTT1KO As(III) is more toxic than As(V) reversing what occurs in the wild-type strain, which probably may be due to a higher overexpression of the *TtMTT5* gene in this strain, while in strain MTT5KD the toxicities of both arsenic ionic forms are similar. A comparison between these two strains shows that MTT1KO is more resistant to As(V) than strain MTT5KD, while this latter is more resistant to As(III) than MTT1KO. This confirms the importance of the *TtMTT5* gene in As(V) resistance.

As previously reported (De Francisco et al., 2017) the basal expression level of the *TtMTT5* gene is much lower than that of the other MT genes and it seems not to be necessary under non-cellular stress conditions. However, expression levels increase quickly and strongly under stress conditions; hence it has been considered as an "alarm" MT gene. In *T. thermophila* adapted strains to high concentrations of Cd or Pb, the *TtMTT5* gene is highly overexpressed compared to the rest of the MT genes of this ciliate. (De Francisco et al., 2018). Similar to Pb or Cd, this *TtMTT5* gene could strongly respond to As(V), an inorganic ion as toxic as them.

5. Conclusions and final remarks

The following general conclusions can be drawn from the results of this research work:

1. The differential toxicity shown by As(III) and As(V) in *T. thermophila* is corroborated by the differences observed both at the level of gene expression of several genes encoding antioxidant enzymes or detoxifying molecules, as well as at the level of cell ultrastructural alterations and ROS/RNS production, despite the fact that both cause a strong and similar mitochondrial dysfunction. Likewise, this study provides cytological and molecular tools to be used as biomarkers for each of the two arsenic ionic forms.
2. For the first time in studies on arsenic, the relevance of metallothioneins in the defense against this metalloid is shown. Metallothioneins play an essential role in counteracting the toxic action of both forms of arsenic, but mainly of As(V). As shown by qRT-PCR results and strains overexpressing MT genes and knockout or knockdown strains in which a MT gene is missing or has a lower copy number than the wild-type strain.
3. *T. thermophila*, with a biology close to mammals, is shown as an important eukaryotic cell model to carry out ecotoxicological studies and as a model to analyze some human diseases driven by processes like ferroptosis and obesity, which may also be caused by/or related to toxic metal(loid)s.

CRediT authorship contribution statement

Daniel Rodríguez-Martín (DRM): Methodology; Formal analysis, Investigation. **Antonio Murciano (AM):** Formal analysis. **Marta Hérraiz (MH):** Investigation. **Patricia De Francisco (PDF):** Investigation. **Francisco Amaro (FA):** Investigation. **Ana Martín-González (AMG):** Conceptualization; Methodology and Writing – review & editing. **Juan Carlos Gutiérrez (JCG):** Conceptualization; Methodology; Writing – review & editing and Funding acquisition. **Silvia Díaz (SD):** Conceptualization; Methodology; Supervision and Writing – original draft.

Declaration of Competing Interest

The authors declare that they have no known competing financial interests or personal relationships that could have appeared to influence the work reported in this paper.

Acknowledgments

This research was funded by the Spanish Ministry of Economy and Competitiveness, Spain, grant number CGL2016-75494-R awarded to JCG.

Credit author statement

SD, AMG and JCG participated in the experimental design and writing of the text. DRM, MH, PdF and FA were involved in different experimental parts of this research work. AM participated in the statistical analysis.

Appendix A. Supporting information

Supplementary data associated with this article can be found in the online version at doi:10.1016/j.jhazmat.2022.128532.

References

Abbas, G., Murtaza, B., Bibi, I., Shahid, M., Niazi, N.K., Khan, M.I., Amjad, M., Hussain Natasha, M., 2018. Arsenic uptake, toxicity, detoxification, and speciation in plants: physiological, biochemical, and molecular aspects. Int. J. Environ. Res. Public Health 15, 59. https://doi.org/10.3390/ijerph15010059.

Ahmed, M.K., Habibullah-Al-Mamun, M., Parvin, E., Akter, M.S., Khan, M.S., 2013. Arsenic induced toxicity and histopathological changes in gill and liver tissue of freshwater fish, tilapia (*Oreochromis mossambicus*). Exp. Toxicol. Pathol. 65, 903–909. https://doi.org/10.1016/j.etp.2013.01.003.

Al-Makishah, N.H., Taleb, M.A., Barakat, M.A., 2020. Arsenic bioaccumulation in arsenic-contaminated soil: a review. Chem. Pap. 74, 2743–2757. https://doi.org/10.1007/s11696-020-01122-4.

Al-Zoughool, M., Bird, M., Rice, J., Baan, R.A., Billard, M., Birkett, N., Krewski, D., Zielinski, J.M., 2019. Development of a database on key characteristics of human carcinogens. J. Toxicol. Environ. Health B Crit. Rev. 22, 264–287. https://doi.org/10.1080/10937404.2019.1642593.

Amaro, F., Turkewitz, A.P., Martín-González, A., Gutiérrez, J.C., 2014. Functional GFP-metallothionein fusion protein from *Tetrahymena thermophila*: a potential whole-cell biosensor for monitoring heavy metal pollution and a cell model to study metallothionein overproduction effects. Biometals 27, 195–205. https://doi.org/10.1007/s10534-014-9704-0.

Bali, A.S., Sidhu, G.P.S., 2021. Arsenic acquisition, toxicity and tolerance in plants - From physiology to remediation: a review. Chemosphere 283, 131050. https://doi.org/10.1016/j.chemosphere.2021.131050.

Balzano, S., Sardo, A., Blasio, M., Bou Chahine, T., Dell'Anno, F., Sansone, C., Brunet, C., 2020. Microalgal metallothioneins and phytochelatins and their potential use in

bioremediation. Front. Microbiol. 11, 517. https://doi.org/10.3389/fmicb.2020.00517.
Benov, L., Sztejnberg, L., Fridovich, I., 1998. Critical evaluation of the use of hydroethidine as a measure of superoxide anion radical. Free Radic. Biol. Med. 25, 826–831. https://doi.org/10.1016/S0891-5849(98)00163-4.
Blajszczak, C., Bonini, M.G., 2017. Mitochondria targeting by environmental stressors: implications for redox cellular signaling. Toxicology 391, 84–89. https://doi.org/10.1016/j.tox.2017.07.013.
Bliss, C., 1935. The calculation of the dosage-mortality curve. Ann. Appl. Biol. 22, 134–167. https://doi.org/10.1111/j.1744-7348.1935.tb07713.x.
Brooks, W.E., 2007. Minerals Yearbook: Arsenic. U.S. Department of the Interior. U.S. Geological Survey.
Burwell, S.M., 2014. Report on carcinogens. U.S. department of health and human services secretary. Res. Triangle Park.
Byeon, E., Choi, B.S., Park, J.C., Kim, M.S., Kim, D.H., Lee, J.S., Lee, Y.H., Jeong, C.B., Hwang, U.K., Hagiwara, A., Lee, J.S., 2021. The genome of the freshwater monogonont rotifer *Brachionus angularis*: Identification of phase I, II, and III detoxification genes and their roles in molecular ecotoxicology. Comp. Biochem. Physiol. Part D. Genom. Proteom. 38, 100821 https://doi.org/10.1016/j.cbd.2021.100821.
Byeon, E., Yoon, C., Lee, J.S., Lee, Y.H., Jeong, C.B., Lee, J.S., Kang, H.M., 2020. Interspecific biotransformation and detoxification of arsenic compounds in marine rotifer and copepod. J. Hazard. Mater. 391, 122196 https://doi.org/10.1016/j.jhazmat.2020.122196.
Carrillo, J.T., Borthakur, D., 2021. Methods for metal chelation in plant homeostasis: review. Plant Physiol. Biochem. 163, 95–107. https://doi.org/10.1016/j.plaphy.2021.03.045.
Chatterjee, S., Sarkar, S., Bhattacharya, S., 2014. Toxic metals and autophagy. Chem. Res. Toxicol. 27 (11), 1887–1900. https://doi.org/10.1021/tx500264s.
Chen, L., Wu, H., Zhao, J., Zhang, W., Zhang, L., Sun, S., Yang, D., Chen, B., Wang, Q., 2018. The role of GST omega in metabolism and detoxification of arsenic in clam *Ruditapes philippinarum*. Aquatic Toxicol., 204, 9–18. https://doi.org/10.1016/j.aquatox.2018.08.016.
Chiarelli, R., Roccheri, M.C., 2012. Heavy metals and metalloids as autophagy inducing agents: focus on cadmium and arsenic. Cells 1, 597–616. https://doi.org/10.3390/cells1030597.
Coelho, D.G., Marinato, C.S., de Matos, De Andrade, H.M., Da Silva, V.M., Santos-Neves, P.H., Araújo, S.C., Oliveira, J.A., 2020. Is arsenite more toxic than arsenate in plants? Ecotoxicology 29, 196–202. https://doi.org/10.1007/s10646-019-02152-9.
Cohen, S., 2018. Lipid droplets as organelles. Int. Rev. Cell. Mol. Biol. 337, 83–110. https://doi.org/10.1016/bs.ircmb.2017.12.007.
Couto, N., Wood, J., Barber, J., 2016. The role of glutathione reductase and related enzymes on cellular redox homoeostasis network. Free Radic. Biol. Med. 95, 27–42. https://doi.org/10.1016/j.freeradbiomed.2016.02.028.
De Francisco, P., Melgar, L.M., Díaz, S., Martín-González, A., Gutiérrez, J.C., 2016. The *Tetrahymena* metallothionein gene family: twenty-one new cDNAs, molecular characterization, phylogenetic study and comparative analysis of the gene expression under different abiotic stressors. BMC Genom. 17, 346. https://doi.org/10.1186/s12864-016-2658-6.
De Francisco, P., Martín-González, A., Turkewitz, A.P., Gutiérrez, J.C., 2017. Extreme metal adapted, knockout and knockdown strains reveal a coordinated gene expression among different Tetrahymena thermophila metallothionein isoforms. PLoSOne 12, e0189076. https://doi.org/10.1371/journal.pone.0189076.
De Francisco, P., Martin-Gonzalez, A., Turkewitz, A.P., Gutierrez, J.C., 2018. Genome plasticity in response to stress in *Tetrahymena thermophila*: selective and reversible chromosome amplification and paralogous expansion of metallothionein genes. Environ. Microbiol. 20, 2410–2421. https://doi.org/10.1111/1462-2920.14251.
De Francisco, P., Martín-González, A., Rodriguez-Martín, D., Díaz, S., 2021. Interactions with arsenic: Mechanisms of toxicity and cellular resistance in eukaryotic microorganisms. Int. J. Environ. Res. Public Health 18, 12226. https://doi.org/10.3390/ijerph182212226.
Dentler, W., 2000. Fixation of *Tetrahymena* cells for electron microscopy. Methods Cell Biol. 62, 323–331. https://doi.org/10.1016/S0091-679X(08)61540-X.
Dhuldhaj, U.P., Yadav, I.C., Singh, S., Sharma, N.K., 2013. Microbial interactions in the arsenic cycle: adoptive strategies and applications in environmental management. In: Whitacre, D. (Ed.), Reviews of Environmental Contamination and Toxicology, (Continuation of Residue Reviews), 224. Springer, New York, NY. https://doi.org/10.1007/978-1-4614-5882-1_1.
Di, X., Beesley, L., Zhang, Z., Zhi, S., Jia, Y., Ding, Y., 2019. Microbial arsenic methylation in soil and uptake and metabolism of methylated arsenic in plants: a review. Int. J. Environ. Res. Public Health 16, 5012. https://doi.org/10.3390/ijerph16245012.
Diaz, S., Martín-González, A., Cubas, L., Ortega, R., Amaro, F., Rodríguez-Martín, D., Gutiérrez, J.C., 2016. High resistance of *Tetrahymena thermophila* to paraquat: Mitochondrial alterations, oxidative stress and antioxidant genes expression. Chemosphere 144, 900–917. https://doi.org/10.1016/j.chemosphere.2015.09.010.
Diaz, S., De Francisco, P., Olsson, S., Aguilera, Á., González-Toril, E., Martín-González, A., 2020. Toxicity, physiological, and ultrastructural effects of arsenic and cadmium on the extremophilic microalga *Chlamydomonas acidophila*. Int. J. Environ. Res. Public Health 17, 1650. https://doi.org/10.3390/ijerph17051650.
Dobritzsch, D., Grancharov, K., Hermsen, C., Krauss, G.J., Schaumlöffel, D., 2020. Inhibitory effect of metals on animal and plant glutathione transferases. J. Trace Elem. Med. Biol. 57, 48–56. https://doi.org/10.1016/j.jtemb.2019.09.007.
Doherty, J., Baehrecke, E.H., 2018. Life, death and autophagy. Nat. Cell Biol. 20 (10), 1110–1117. https://doi.org/10.1038/s41556-018-0201-5.
Espart, A., Marín, M., Gil-Moreno, S., Palacios, Ò., Amaro, F., Martín-González, A., Gutiérrez, J.C., Capdevila, M., Atrian, S., 2015. Hints for metal-preference protein sequence determinants: different metal binding features of the five *Tetrahymena thermophila* metallothioneins. Int. J. Biol. Sci. 11, 456–471. https://doi.org/10.7150/ijbs.11060.
Eze, C.T.-G., Michelangeli, F., Otitoloju, A.A., 2019. In vitro cyto-toxic assessment of heavy metals and their binary mixtures on mast cell-like, rat basophilic leukemia (RBL-2H3) cells. Chemosphere 223, 686–693. https://doi.org/10.1016/j.chemosphere.2019.02.035.
Fan, W.H., Ren, J.Q., Li, X.M., Wei, C.Y., Xue, F., Zhang, N., 2015. Bioaccumulation and oxidative stress in *Daphnia magna* exposed to arsenite and arsenate. Environ. Toxicol. Chem. 34, 2629–2635. https://doi.org/10.1002/etc.3119.
Fei, D., Zhao, H., Wang, Y., Liu, J., Mu, M., Guo, M., Yang, X., Xing, M., 2019. The disturbance of autophagy and apoptosis in the gizzard caused by copper and/or arsenic are related to mitochondrial kinetics. Chemosphere 231, 1–9. https://doi.org/10.1016/j.chemosphere.2019.05.101.
Finnegan, P.M., Chen, W., 2012. Arsenic toxicity: the effects on plant metabolism. Front. Physiol. 3, 182. https://doi.org/10.3389/fphys.2012.00182.
Flora, S.J., 2011. Arsenic-induced oxidative stress and its reversibility. Free Radic. Biol. Med. 51, 257–281.
Flora, S.J., Flora, G., Saxena, G., Mishra, M., 2007. Arsenic and lead induced free radical generation and their reversibility following chelation. Cell. Mol. Biol. 53, 26–47.
Fowler, B.A., Woods, J.S., Schiller, C.M., 1977. Ultrastructural and biochemical effects of prolonged oral arsenic exposure on liver mitochondria of rats. Environ. Health Perspect. 19, 197–204. https://doi.org/10.1289/ehp.7719197.
Fu, Y., Wang, L., Peng, W., Fan, Q., Li, Q., Dong, Y., Liu, Y., Boczkaj, G., Wang, Z., 2021. Enabling simultaneous redox transformation of toxic chromium(VI) and arsenic(III) in aqueous media: a review. J. Hazard. Mater. 417, 126041 https://doi.org/10.1016/j.jhazmat.2021.126041.
Garbinski, L.D., Rosen, B.P., Chen, J., 2019. Pathways of arsenic uptake and efflux. Environ. Int. 126, 585–597. https://doi.org/10.1016/B978-0-12-394390-3.00012-4.
Garza-Lombó, C., Pappa, A., Panayiotidis, M.I., Franco, R., 2020. Redox homeostasis, oxidative stress and mitophagy. Mitochondrion 51, 105–117. https://doi.org/10.1016/j.mito.2020.01.002.
Gomes, A., Fernández, E., Lima, J.L., 2005. Fluorescence probes used for detection of reactive oxygen species. J. Biochem. Biophys. Methods 65, 45–80. https://doi.org/10.1016/j.jbbm.2005.10.003.
Guidarelli, A., Fiorani, M., Cerioni, L., Cantoni, O., 2019. The compartmentalised nature of the mechanisms governing superoxide formation and scavenging in cells exposed to arsenite. Toxicol. Appl. Pharmacol. 384, 114766 https://doi.org/10.1016/j.taap.2019.114766.
Gutierrez, J.C., Martin-Gonzalez, A., Callejas, S., 1998. Nuclear changes, macronuclear chromatin reorganization and DNA modifications during ciliate encystment. Eu. J. Protistol. 34, 97–103.
Gutierrez, J.C., Martin-Gonzalez, A., Diaz, S., Amaro, F., Ortega, R., Gallego, A., de Lucas, M.P., 2008. Ciliates as cellular tools to study the eukaryotic cell-heavy metals interactions. In: Brown, S.E., Welton, W.C. (Eds.), Heavy Met. Pollut. Nova Sci., N. Y., Publ. Inc. 1–44.
Gutierrez, J.C., De Francisco, P., Amaro, F., Díaz, S., Martín-González, A., 2019. Structural and functional diversity of microbial metallothionein genes. In: Surajit Das, S., Dash, H.R. (Eds.), Microbial Diversity in The Genomic Era. Academic Press, pp. 387–407. https://doi.org/10.1016/B978-0-12-814849-5.00022-8.
Gutu, C.M., Olaru, O.T., Purdel, N.C., Ilie, M., Diacu, E., 2015. Phytotoxicity of inorganic arsenic assessed by Triticum test. Rev. Chim. 66, 333–335.
Hayes, J.D., Flanagan, J.U., Jowsey, I.R., 2005. Glutathione transferases. Annu. Rev. Pharmacol. Toxicol. 45, 51–88.
He, W., Megharaj, M., Naidu, R., 2009. Toxicity of tri- and penta-valent arsenic, alone and in combination, to the cladoceran *Daphnia carinata*: the influence of microbial transformation in natural waters. Environ. Geochem. Health 31, 133–141. https://doi.org/10.1007/s10653-008-9239-9.
Hirano, S., 2020. Biotransformation of arsenic and toxicological implication of arsenic metabolites. Arch. Toxicol. 94 (8) https://doi.org/10.1007/s00204-020-02772-9.
Hu, Y., Li, J., Lou, B., Wu, R., Wang, G., Lu, C., Wang, H., Pi, J., Xu, Y., 2020. The role of reactive oxygen species in arsenic toxicity. Biomolecules 10, 240. https://doi.org/10.3390/biom10020240.
Hughes, M.F., 2002. Arsenic toxicity and potential mechanisms of action. Toxicol. Lett. 133, 1–16.
Irvine, G.W., Tan, S.N., Stillman, M.J., 2017. A simple metallothionein-based biosensor for enhanced detection of arsenic and mercury. Biosensors 7, 14. https://doi.org/10.3390/bios7010014.
Jomova, K., Jenisova, Z., Feszterova, M., Baros, S., Liska, J., Hudecova, D., Rhodes, C.J., Valko, M., 2011. Arsenic: toxicity, oxidative stress and human disease. J. Appl. Toxicol. 31, 95–107. https://doi.org/10.1002/jat.1649.
Jomova, K., Valko, M., 2011. Advances in metal-induced oxidative stress and human disease. Toxicology 283, 65–87. https://doi.org/10.1016/j.tox.2011.03.001.
Kalyanaraman, B., Dranka, B.P., Hardy, M., Michalski, R., Zielonka, J., 2014. HPLC-based monitoring of products formed from hydroethidine-based fluorogenic probes–the ultimate approach for intra- and extracellular superoxide detection. Biochim Biophys. Acta 1840, 739–744.
Karadjova, I.B., Slaveykova, V.I., Tsalev, D.L., 2008. The biouptake and toxicity of arsenic species on the green microalga *Chlorella salina* in seawater. Aquat. Toxicol. 87, 264–271. https://doi.org/10.1016/j.aquatox.2008.02.006.
Karri, V., Kumar, V., Ramos, D., Oliveira, E., Schuhmacher, M., 2018. Comparative in vitro toxicity evaluation of heavy metals (lead, cadmium, arsenic, and methylmercury) on HT-22 hippocampal cell line. Biol. Trace Elem. Res. 184, 226–239. ⟨https://link.springer.com/article/10.1007%2Fs12011-017-1177-x⟩.

Kaur, H., Sparvoli, D., Osakada, H., Iwamoto, M., Haraguchi, T., Turkewitz, A.P., 2017. An endosomal syntaxin and the AP-3 complex are required for formation and maturation of candidate lysosome-related secretory organelles (mucocysts) in *Tetrahymena thermophila*. Mol. Biol. Cell. 28, 1551–1564. https://doi.org/10.1091/mbc.E17-01-0018.

Kilpi-Koski, J., Penttinen, O.P., Väisänen, A.O., van Gestel, C.A.M., 2020. Toxicity of binary mixtures of Cu, Cr and As to the earthworm *Eisenia andrei*. Ecotoxicology 29, 900–911. https://doi.org/10.1007/s10646-020-02240-1.

Kotiadis, V.N., Duchen, M.R., Osellame, L.D., 2014. Mitochondrial quality control and communications with the nucleus are important in maintaining mitochondrial function and cell health. Biochim. Biophys. Acta 1840, 1254–1265. https://doi.org/10.1016/j.bbagen.2013.10.041.

Kotze, A.A., Tuffin, I.M., Deane, S.M., Rawlings, D.E., 2006. Cloning and characterization of the chromosomal arsenic resistance genes from *Acidithiobacillus caldus* and enhanced arsenic resistance on conjugal transfer of ars genes located on transposon TnAtcArs. Microbiology 152, 3551–3560. https://doi.org/10.1099/mic.0.29247-0.

Kumar, M., Lalit, M., Thakur, R., 2016. Natural antioxidants against arsenic-induced genotoxicity. Biol. Trace Elem. Res. 170, 84–93. https://doi.org/10.1007/s12011-015-0448-7.

Kumari, A., Pandey, N., Pandey-Rai, S., 2018. Exogenous salicylic acid-mediated modulation of arsenic stress tolerance with enhanced accumulation of secondary metabolites and improved size of glandular trichomes in *Artemisia annua L.* Protoplasma 255, 139–152.

Larionov, A., Krause, A., Miller, W., 2005. A standard curve based method for relative real time PCR data processing. BMC Bioinforma. 6, 62. https://doi.org/10.1186/1471-2105-6-62.

Lei, P., Bai, T., Sun, Y., 2019. Mechanisms of ferroptosis and relations with regulated cell death: a review. Front. Physiol. 10, 139. https://doi.org/10.3389/fphys.2019.00139.

Leong, Y.K., Chang, J.S., 2020. Bioremediation of heavy metals using microalgae: recent advances and mechanisms. Bioresour. Technol. 303, 122886.

Levy, J.L., Stauber, J.L., Adams, M.S., Maher, W.A., Kirby, J.K., Jolley, D.F., 2005. Toxicity, biotransformation, and mode of action of arsenic in two freshwater microalgae (*Chlorella sp.* and *Monoraphidium arcuatum*). Environ. Toxicol. Chem. 24, 2630–2639. https://doi.org/10.1897/04-580R.1.

Li, J., Cao, F., Yin, H.-L., Huang, Z.-J., Lin, Z.-T., Mao, N., Sun, B., Wang, G., 2020. Ferroptosis: past, present and future. Cell Death Dis. 11, 88. https://doi.org/10.1038/s41419-020-2298-2.

Li, S., Zhao, H., Wang, Y., Shao, Y., Wang, B., Wang, Y., Xing, M., 2018. Regulation of autophagy factors by oxidative stress and cardiac enzymes imbalance during arsenic or/and copper induced cardiotoxicity in *Gallus gallus*. Ecotoxicol. Environ. Saf. 148, 125–134. https://doi.org/10.1016/j.ecoenv.2017.10.018.

Lu, J., Holmgren, A., 2014. The thioredoxin antioxidant system. Free Radic. Biol. Med. 66, 75–87. https://doi.org/10.1016/j.freeradbiomed.2013.07.036.

Luz, A.L., Godebo, T.R., Smith, L.L., Leuthner, T.C., Maurer, L.L., Meyer, J.N., 2017. Deficiencies in mitochondrial dynamics sensitize *Caenorhabditis elegans* to arsenite and other mitochondrial toxicants by reducing mitochondrial adaptability. Toxicology 387, 81–94. https://doi.org/10.1016/j.tox.2017.05.018.

Lynn, S., Gurr, J.R., Lai, H.T., Jan, K.Y., 2000. NADH oxidase activation is involved in arsenite-induced oxidative DNA damage in human vascular smooth muscle cells. Circ. Res. 85, 514–519. https://doi.org/10.1161/01.RES.86.5.514.

Maciaszczyk-Dziubinska, E., Wawrzycka, D., Wysocki, R., 2012. Arsenic and antimony transporters in eukaryotes. Int. J. Mol. Sci. 13, 3527–3548. https://doi.org/10.3390/ijms13033527.

Mandal, B.K., Suzuki, K.T., 2002. Arsenic round the world: a review. Talanta 58, 201–235. https://doi.org/10.1016/S0039-9140(02)00268-0.

Martin, O., Scholze, M., Ermler, S., McPhie, J., Bopp, S.K., Kienzler, A., Parissis, N., Kortenkamp, A., 2021. Ten years of research on synergisms and antagonisms in chemical mixtures: A systematic review and quantitative reappraisal of mixture studies. Environ. Int. 146, 160–4120. https://doi.org/10.1016/j.envint.2020.106206.

Martin-Gonzalez, A., Borniquel, S., Díaz, S., Ortega, R., Gutierrez, J.C., 2005. Ultrastructural alterations in ciliated protozoa under heavy metal exposure. Cell Biol. Int 29 (119), e126. https://doi.org/10.1016/j.cellbi.2004.09.010.

Mazumder, P., Sharma, S.K., Taki, K., Kalamdhad, A.S, Kumar, M., 2020. Microbes involved in arsenic mobilization and respiration: a review on isolation, identification, isolates and implications. Environ. Geochem. Health. https://doi.org/10.1007/s10653-020-00549-8.

Meharg, A.A., Raab, A., 2010. Getting to the bottom of arsenic standards and guidelines. Environ. Sci. Technol. 44, 4395–4399. https://doi.org/10.1021/es9034304.

Meng, P., Zhang, S., Jiang, X., Cheng, S., Zhang, J., Cao, X., Qin, X., Zou, Z., Chen, C., 2020. Arsenite induces testicular oxidative stress in vivo and in vitro leading to ferroptosis. Ecotoxicol. Environ. Saf. 194, 110360 https://doi.org/10.1016/j.ecoenv.2020.110360.

Miazek, K., Iwanek, W., Remacle, C., Richel, A., Goffin, D., 2015. Effect of metals, metalloids and metallic nanoparticles on microalgae growth and industrial product biosynthesis: a review. Int. J. Mol. Sci. 16, 23929–23969. https://doi.org/10.3390/ijms161023929.

Miller, C.G., Holmgren, A., Arner, E.S.J., Schmidt, E.E., 2018. NADPH-dependent and –independent disulfide reductase systems. Free Radic. Biol. Med. 1, 248–261. https://doi.org/10.1016/j.freeradbiomed.2018.03.051.

Minatel, B.C., Sage, A.P., Anderson, C., Hubaux, R., Marshall, E.A., Lam, W.L., Martinez, V.D., 2018. Environmental arsenic exposure: from genetic susceptibility to pathogenesis. Environ. Int. 112, 183–197. https://doi.org/10.1016/j.envint.2017.12.017.

Muenyi, C.S., Ljungman, M., States, J.C., 2015. Arsenic disruption of DNA damage responses: potential role in carcinogenesis and chemotherapy. Biomolecules 5, 2184–2193. https://doi.org/10.3390/biom5042184.

Mukhopadhyay, R., Rosen, B.P., 2002. Arsenate reductases in prokaryotes and eukaryotes. Environ. Heal. Perspect. 110, 745–748. https://doi.org/10.1289/ehp.02110s5745.

Muthumani, M., Miltonprabu, S., 2015. Ameliorative efficacy of tetrahydrocurcumin against arsenic induced oxidative damage, dyslipidemia and hepatic mitochondrial toxicity in rats. Chem. Biol. Interact. 235, 95–105. https://doi.org/10.1016/j.cbi.2015.04.006.

Nagvenkar, G.S., Ramaiah, N., 2010. Arsenite tolerance and biotransformation potential in estuarine bacteria. Ecotoxicology 19, 604–613. https://doi.org/10.1007/s10646-009-0429-8.

Ngu, T.T., Stillman, M.J., 2006. Arsenic binding to human metallothionein. J. Am. Chem. Soc. 128, 12473–12483.

Nurchi, V.N., Djordjevic, A.B., Crisponi, G., Alexander, J., Bjørklund, G., Aaseth, J., 2020. Arsenic toxicity: molecular targets and therapeutic agents. Biomolecules 10, 235. https://doi.org/10.3390/biom10020235.

Ordoñez, E., Letek, M., Valbuena, N., Gil, J.A., Mateos, L.M., 2005. Analysis of genes involved in arsenic resistance in *Corynebacterium glutamicum* ATCC 13032. Appl. Environ. Microbiol. 71, 6206–6215. https://doi.org/10.1128/AEM.71.10.6206-6215.2005.

Ozturk, M., Metin, M., Altay, V., Bhat, R.A., Ejaz, M., Gul, A., Unal, B.T., Hasanuzzama, M., Nibir, L., Nahar, K., Bukhari, A., Dervash, M.A., Kawano, T., 2021. Arsenic and human health: genotoxicity, epigenomic effects, and cancer signaling. Biol. Trace Elem. Res. https://doi.org/10.1007/s12011-021-02719-w.

Pan, Y., Zhu, M., Wang, S., Ma, G., Huang, X., Qiao, C., Wang, R., Xu, X., Liang, Y., Lu, K., Li, J., Qu, C., 2018. Genome-wide characterization and analysis of metallothionein family genes that function in metal stress tolerance in *Brassica napus* L. Int. J. Mol. Sci. 19, 2181. https://doi.org/10.3390/ijms19082181.

Phaniendra, A., Jestadi, D.B., Periyasamy, L., 2015. Free radicals: properties, sources, targets, and their implication in various diseases. Indian J. Clin. Biochem 30, 11–26. https://doi.org/10.1007/s12291-014-0446-0.

Pawlik-Skowrońska, B., Pirszel, J., Kalinowska, R., Skowroński, T., 2004. Arsenic availability, toxicity and direct role of GSH and phytochelatins in As detoxification in the green alga *Stichococcus bacillaris*. Aquatic Toxicol 201–212. https://doi.org/10.1016/j.aquatox.2004.09.003.

Pfaffl, M.W., Horgan, G.W., Dempfle, L., 2002. Relative expression software tool (REST©) for group-wise comparison and statistical analysis of relative expression results in real-time PCR. Nucleic. Acid. Res. 30, e36 https://doi.org/10.1093/nar/30.9.e36.

Piccinni, E., Irato, P., Coppellotti, O., Guidolin, L., 1987. Biochemical and ultrastructural data on *Tetrahymena pyriformis* treated with copper and cadmium. J. Cell Sc. 88, 283–293.

Prakash, C., Chhikara, S., Kumar, V., 2021. Mitochondrial dysfunction in arsenic-induced hepatotoxicity: pathogenic and therapeutic implications. Biol. Trace Elem. Res. https://doi.org/10.1007/s12011-021-02624-2.

Prakash, C., Soni, M., Kumar, V., 2015. Biochemical and molecular alterations following arsenic-induced oxidative stress and mitochondrial dysfunction in rat brain. Biol. Trace Elem. Res. 167, 121–129. ⟨https://link.springer.com/article/10.1007%2Fs12011-015-0284-9⟩.

Prakash, C., Soni, M., Kumar, V., 2016. Mitochondrial oxidative stress and dysfunction in arsenic neurotoxicity: a review. J. Appl. Toxicol. 36, 179–188. https://doi.org/10.1002/jat.3256.

Rahman, M.A., Hassler, C., 2014. Is arsenic biotransformation a detoxification mechanism for microorganisms? Aquat. Toxicol. 146, 212–219. https://doi.org/10.1016/j.aquatox.2013.11.009.

Rahman, M.A., Hogan, B., Duncan, D., Doyle, C., Krassoi, R., Rahman, M.M., Naidu, R., Lim, R.P., Maher, W., Hassler, C., 2014. Toxicity of arsenic species to three freshwater organisms and biotransformation of inorganic arsenic by freshwater phytoplankton (*Chlorella* sp. CE-35). Ecotoxicol. Environ. Saf. 106, 126–135. https://doi.org/10.1016/j.ecoenv.2014.03.004.

Rhaman, M.T., De Ley, M., 2017. Arsenic induction of metallothionein and metallothionein induction against arsenic cytotoxicity. Rev. Environ. Contam. Toxicol. 240, 151–168. https://doi.org/10.1007/398_2016_2.

Romero, I., de Francisco, P., Gutiérrez, J.C., Martín-González, A., 2019. Selenium cytotoxicity in *Tetrahymena thermophila*: new clues about its biological effects and cellular resistance mechanisms. Sci. Total Environ. 671, 850–865. https://doi.org/10.1016/j.scitotenv.2019.03.115.

Rosati, G., Modeo, L., 2003. Extrusomes in ciliates: diversification, distribution, and phylogenetic implications. J. Eukaryot. Microbiol. 50, 383–402. https://doi.org/10.1111/j.1550-7408.2003.tb00260.x.

Roy, J.S., Chatterjee, D., Das, N., Giri, A.K., 2018. Substantial evidences indicate that inorganic arsenic is a genotoxic carcinogen: a review. Toxicol. Res 34, 311–324. https://doi.org/10.5487/TR.2018.34.4.311.

Saha, J., Majumder, B., Mumtaz, B., Biswas, A.K., 2017. Arsenic-induced oxidative stress and thiol metabolism in two cultivars of rice and its possible reversal by phosphate. Acta Physiol. Plant. 39, 263. https://doi.org/10.1007/s11738-017-2562-y.

Sambrook, J., Russell, D.W., 2006. Purification of nucleic acids by extraction with phenol: chloroform. CSH Protoc., pdb. prot4455. https://doi.org/10.1101/pdb.prot4455.

Schott, M., Weller, S., Schulze, R., Krueger, E., Drizyte-Miller, K., Casey, C., McNiven, M., 2019. Lipid droplet size directs lipolysis and lipophagy catabolism in hepatocytes. J. Cell Biol. 218. https://doi.org/10.1083/jcb.201803153.

Shaji, E., Santosh, M., Sarath, K.V., Prakash, P., Deepchand, V., Divya, B.V., 2021. Arsenic contamination of groundwater: a global synopsis with focus on the Indian Peninsula. Geosci. Front. 12. https://doi.org/10.1016/j.gsf.2020.08.015.

Shakya, S., Pradhan, B., Smith, L., Shrestha, J., Tuladhar, S., 2012. Isolation and characterization of aerobic culturable arsenic-resistant bacteria from surfacewater and groundwater of Rautahat District, Nepal. J. Environ. Manag. 95, S250–S255. https://doi.org/10.1016/j.jenvman.2011.08.001.

Sharma, V.K., Sohn, M., 2009. Aquatic arsenic: toxicity, speciation, transformations, and remediation. Environ. Int. 35, 743–759. https://doi.org/10.1016/j.envint.2009.01.005.

Shaw, J.R., Glaholt, S.P., Greenberg, N.S., Sierra-Alvarez, R., Folt, C.L., 2007. Acute toxicity of arsenic to *Daphnia pulex*: influence of organic functional groups and oxidation state. Environ. Toxico. Chem. 26, 1532–1537. https://doi.org/10.1897/06-389R.1.

Shi, H., Shi, X., Liu, K.J., 2004. Oxidative mechanism of arsenic toxicity and carcinogenesis. Mol. Cell Biochem. 255, 67–78. https://doi.org/10.1023/b:mcbi.0000007262.26044.e8.

Sies, H., Jones, D.P., 2020. Reactive oxygen species (ROS) as pleiotropic physiological signalling agents. Nat. Rev. Mol. Cell Biol. 21, 363–383. https://doi.org/10.1038/s41580-020-0230-3.

Souza, A.C.F., De Paiva Coimbra, J.L., Ervilha, L.O.G., Bastos, D.D.S., Cossolin, J.F.S., Santos, E.C., de Oliveira, L.L., Machado-Neves, M., 2020. Arsenic induces dose-dependent structural and ultrastructural pathological remodeling in the heart of Wistar rats. Life Sci. 257, 118132 https://doi.org/10.1016/j.lfs.2020.118132.

Sprague, J.B., 1970. Measurements of pollutants toxicity to fish II. Utilizing and applying bioassay results. Water Res. 4, 3–32.

Stolz, J.F., Basu, P., Santini, J.M., Oremland, R.S., 2006. Arsenic and selenium in microbial metabolism. Annu. Rev. Microbiol. 60, 107–130. https://doi.org/10.1146/annurev.micro.60.080805.142053.

Stolz, J.F., Basu, P., Oremland, R.S., 2002. Microbial transformation of elements: the case of arsenic and selenium. Int. Microbiol. 5, 201–207. https://doi.org/10.1007/s10123-002-0091-y.pdf. ⟨https://link.springer.com/content/pdf/⟩.

Stýblo, M., Venkatratnam, A., Fry, R.C., Thomas, D.J., 2021. Origins, fate, and actions of methylated trivalent metabolites of inorganic arsenic: progress and prospects. Arch. Toxicol. 95, 1547–1572. https://doi.org/10.1007/s00204-021-03028-w.

Sun, J., Cheng, J., Yang, Z., Li, K., Zhou, J., Cen, K., 2015. Microstructures and functional groups of *Nannochloropsis* sp. cells with arsenic adsorption and lipid accumulation. Bioresour. Technol. 194, 305–311. https://doi.org/10.1016/j.biortech.2015.07.041.

Tam, L.M., Wang, Y., 2020. Arsenic exposure and compromised protein quality control. Chem. Res. Toxicol. 33, 1594–1604. https://doi.org/10.1021/acs.chemrestox.0c00107.

Tam, L.M., Price, N.E., Wang, Y., 2020. Molecular mechanisms of arsenic-induced disruption of DNA repair. Chem. Res. Toxicol. 33, 709–726. https://doi.org/10.1021/acs.chemrestox.9b00464.

Thomas, D.J., 2007. Molecular processes in cellular arsenic metabolism. Toxicol. Appl. Pharmacol. 222, 365–373. https://doi.org/10.1016/j.taap.2007.02.007.

Thomas, D.J., 2021. Arsenic methylation. Lessons three Decades Res. Toxicol. 457, 152800 https://doi.org/10.1016/j.tox.2021.152800.

Tinkov, A.A., Aschner, M., Ke, T., Ferrer, B., Zhou, J.C., Chang, J.S., Santamaría, A., Chao, J.C., Aaseth, J., Skalny, A.V., 2021. Adipotropic effects of heavy metals and their potential role in obesity. Fac. Rev. 10, 32. https://doi.org/10.12703/r/10-32.

Tripathi, R.D., Tripathi, P., Dwivedi, S., Dubey, S., Chatterjee, S., Chakrabarty, D., Trivedi, P.K., 2012. Arsenomics: omics of arsenic metabolism in plants. Front. Physiol. 3, 275. https://doi.org/10.3389/fphys.2012.00275.

Tsai, S.L., Singh, S., Chen, W., 2009. Arsenic metabolism by microbes in nature and the impact on arsenic remediation. Curr. Opin. Biotech. 20, 659–667. https://doi.org/10.1016/j.copbio.2009.09.013.

Valko, M., Jomova, K., Rhodes, C.J., Kuca, K., Musílek, K., 2016. Redox-and non-redox-metal-induced formation of free radicals and their role in human disease. Arch. Toxicol. 90, 1–37. ⟨https://link.springer.com/article/10.1007%2Fs00204-015-1579-5⟩.

Vellinger, C., Parant, M., Rousselle, P., Usseglio-Polatera, P., 2012. Antagonistic toxicity of arsenate and cadmium in a freshwater amphipod (*Gammarus pulex*). Ecotoxicology 7, 1817–1827. https://doi.org/10.1007/s10646-012-0916-1.

Walker, C.H., Sibly, R.M., Hopkins, S.P., Peakall, D.B., 2012. Principles of Ecotoxicology, fourth ed. CRC Press (Taylor and Francis),, Boca Raton.

Wang, N.X., Liu, Y.Y., Wei, Z.B., Yang, L.Y., Miao, A.J., 2018. Waterborne and diet borne toxicity of inorganic arsenic to the freshwater zooplankton *Daphnia magna*. Environ. Sci. Technol. 52 (15), 8912–8919. https://doi.org/10.1021/acs.est.8b02600.

Wei, S., Qiu, T., Yao, X., Wang, N., Jiang, L., Jia, X., Tao, Y., Wang, Z., Pei, P., Zhang, J., Zhu, Y., Yang, G., Liu, X., Liu, S., Sun, X., 2020. Arsenic induces pancreatic dysfunction and ferroptosis via mitochondrial ROS-autophagy-lysosomal pathway. J. Hazard. Mater. 384, 121390 https://doi.org/10.1016/j.jhazmat.2019.121390.

Winterbourn, C.C., Parsons-Mair, H.N., Gebicki, S., Gebicki, J.M., Davies, M.J., 2004. Requirements for superoxide-dependent tyrosine hydroperoxide formation in peptides. Biochem. J. 381 (1), 241–248. https://doi.org/10.1042/BJ20040259.

World Health Organization (WHO), 2011. Guidelines for drinking-water quality, 4th ed. ISBN 9789241548151. ⟨https://apps.who.int/iris/handle/10665/44584⟩.

Wu, X., Hu, J., Wu, F., Zhang, X., Wang, B., Yang, Y., Shen, G., Liu, J., Tao, S., Wang, X., 2021. Application of TiO_2 nanoparticles to reduce bioaccumulation of arsenic in rice seedlings (*Oryza sativa L.*): a mechanistic study. J. Hazard. Mater. 405, 124047 https://doi.org/10.1016/j.jhazmat.2020.124047.

Yao, X.F., Zheng, B.L., Bai, J., Jiang, L.P., Zheng, Y., Qi, B.X., Geng, C.Y., Zhong, L.F., Yang, G., Chen, M., Liu, X.F., Sun, X.C., 2015. Low-level sodium arsenite induces apoptosis through inhibiting TrxR activity in pancreatic β-cells. Environ. Toxicol. Pharmacol. 40 (2), 486–491. https://doi.org/10.1016/j.etap.2015.08.003.

Ye, J., Chang, Y., Yan, Y., Xiong, J., Xue, X.-M., Yuan, D., Sun, G.-X., Zhu, Y.-G., Miao, W., 2014. Identification and characterization of the arsenite methyltransferase from a protozoan*Tetrahymena pyriformis*. Aquat. Toxicol. 149, 50–57.

Ye, Q., Feng, Y., Wang, Z., Jiang, W., Qu, Y., Zhang, C., Zhou, A., Xie, S., Zou, J., 2018. Effects of gelsemine on oxidative stress and DNA damage responses of *Tetrahymena thermophila*. PeerJ 6, e6093. https://doi.org/10.7717/peerj.6093.

Yin, X.-X., Zhang, Y.-Y., Yang, J., Zhu, Y.-G., 2011. Rapid biotransformation of arsenic by a model protozoan *Tetrahymena thermophila*. Environ. Poll 159, 837–840. https://doi.org/10.1016/jenvpol.2010.12.033.

Yoo, J.W., Cho, H., Lee, K.W., Won, E.J., Lee, Y.M., 2021. Combined effects of heavy metals (Cd, As, and Pb): comparative study using conceptual models and the antioxidant responses in the brackish water flea. Comp. Biochem. Physiol. C Toxicol. Pharmacol. 239, 108863 https://doi.org/10.1016/j.cbpc.2020.108863.

Yousuf, P.Y., Hakeem, K.U. R., Chandna, R., Ahmad, P., 2012. Role of Glutathione Reductase in Plant Abiotic Stress, in: Ahmad, P. and Prasad, M.N.V. (Eds.), Abiotic Stress Responses in Plants, pp. 149–158. ⟨https://doi.org/10.1007/978–1-4614–0634-1_8⟩.

Zeinvand-Lorestani, M., Kalantari, H., Khodayar, M.J., Teimoori, A., Saki, N., Ahangarpour, A., Rahim, F., Khorsandi, L., 2018. Dysregulation of Sqstm1, mitophagy, and apoptotic genes in chronic exposure to arsenic and high-fat diet (HFD). Environ. Sci. Pollut. Res. Int. 25 (34), 34351–34359. https://doi.org/10.1007/s11356-018-3349-4.

Zhang, J.Y., Ding, T.D., Zhang, C.L., 2013a. Biosorption and toxicity responses to arsenite (As(III)) in *Scenedesmus quadricauda*. Chemosphere 92, 1077–1084. https://doi.org/10.1016/j.chemosphere.2013.01.002.

Zhang, J.Y., Sun, G.X., Rensing, C., Zhu, Y.G., 2013b. Biomethylation and volatilization of arsenic by the marine microalgae *Ostreococcus tauri*. Chemosphere 93, 47–53. https://doi.org/10.1016/j.chemosphere.2013.04.063.

Zhang, Y.Y., Yang, J., Yin, X.X., Yang, S.P., Zhu, Y.G., 2012. Arsenate toxicity and stress responses in the freshwater ciliate *Tetrahymena pyriformis*. Eur. J. Protistol. 48 (3), 227–236. https://doi.org/10.1016/j.ejop.2012.01.005.

Zhang, Z., Pratheeshkumar, P., Budhraja, A., Son, Y.-O., Kim, D., Shi, X., 2015. Role of reactive oxygen species in arsenic-induced transformation of human lung bronchial epithelial (BEAS-2B) cells. Biochem. Biophys. Res. Commun. 456 (2), 643–648. https://doi.org/10.1016/j.bbrc.2014.12.010.

Zhao, R., Xie, C.T., Xu, Y., Ji, D.H., Chen, C.S., Ye, J., Xue, X.M., Wang, W.L., 2020. The response of *Pyropia haitanensis* to inorganic arsenic under laboratory culture. Chemosphere 261, 128160. https://doi.org/10.1016/j.chemosphere.2020.128160.